이학박사학위논문

예쁜꼬마선충 유전학을 이용한 Hippo pathway의 새로운 생물학적 기능 규명 연구

Genetic and Functional Dissection of the Hippo Pathway in *Caenorhabditis elegans*

2017년 8월

서울대학교 대학원

생명과학부

이 하 늬

ABSTRACT

Genetic and Functional Dissection of the Hippo Pathway in *Caenorhabditis elegans*

Hanee Lee

Dept. of Biological Sciences

The Graduate School

Seoul National University

The Hippo (Hpo) pathway is a conserved signaling pathway which has essential roles in early development of organisms. It regulates organ size homeostasis via controlling cell proliferation and apoptosis and mediates polarized cell differentiation. In *Caenorhabditis elegans*, although several components of the Hpo pathway and genetic interactions among them were reported, the physiological functions of the Hpo pathway are relatively unknown. Here, using many genetic approaches, I elucidated that the conserved Hpo pathway functions in the apicobasal polarity maintenance of growing intestinal membrane and the maintenance of structural integrity of neurons in *C. elegans*.

In polarized epithelial cells, functionally distinct membrane domains are established and tightly maintained during development. Although many conserved polarity determinants have been identified, the mechanism to maintain the apicobasal polarity in expanding membranes is not yet fully understood. From genetic screenings, I delineated the conserved NFM-1-WTS-1-YAP-1 signaling cascade plays a role in the maintenance of apicobasal polarity by regulating a conserved P-type ATPase, *tat-2*. The Hpo pathway-mediated *tat-2* regulation is important to maintain apicobasal membrane identities, which leads to polarized sorting of newly synthesized proteins in the expanding membrane.

I also defined neuronal roles of the Hpo pathway in *C. elegans*. I found that *yap-1*, the worm homolog of YAP/Yki, acts in asymmetric development of neurons. In addition to its functions in neuronal development, I found that the Hpo pathway is required to maintain structural integrity of neurons. I observed that worms which lack the Hpo pathway and the Wnt pathway showed defects in neurons such that the mutant exhibited disintegrated neurons precociously. Considering that structural and functional decline of neurons is a hallmark of neuronal aging, my works will provide a molecular mechanism for neuronal aging.

In summary, I report the developmental functions of the Hpo pathway in *C. elegans* intestine and neurons, and the post developmental roles of the Hpo pathway in the structural maintenance of neurons.

Keywords: *C. elegans*, the Hpo pathway, apicobasal polarity, TAT-2, structural integrity of neurons, the Wnt pathway

Student Number: 2009-20352

TABLE OF CONTENTS

LIST OF FIGURES

LIST OF TABLES

Introduction

The roles of the Hippo kinase pathway in early development

The Hippo kinase (Hpo) pathway is a highly conserved signaling pathway present in a range of animals, from flies to mammals; it is known to regulate tissue size homeostasis. During development, when cell number reaches a certain threshold, the Hpo pathway is activated, and LATS/Warts kinase phosphorylates the transcriptional co-activator YAP/Yki and inhibits its nuclear localization. In the nucleus, YAP/Yki interacts with the transcriptional factor TEAD/Sd and regulates the expression of several target genes involved mainly in apoptosis and cell proliferation. The Hpo pathway is also known to regulate cell polarization. In *Drosophila melanogaster*, it has been shown to regulate apical domain size in a manner independent of its functions in controlling organ size (Genevet et al., 2009; Hamaratoglu et al., 2009). In yeasts, a LATS kinase homolog, *orb6*, is also required to maintain cell polarity (Verde et al., 1998).

Apicobasal polarity maintenance in expanding membrane

The polarized plasma membrane of epithelial cells is functionally subdivided into the apical and basolateral membrane domains. These membrane domains are

structurally distinct and the establishment and the maintenance of this polarity during development are essential for organismal survival. Evolutionarily conserved polarity determinants including PAR-aPKC complex proteins have been identified by genetic screening (Hung and Kemphues, 1999; Izumi et al., 1998; Kuchinke et al., 1998; Lin et al., 2000; Tabuse et al., 1998; Wodarz et al., 1999). These membrane-associated proteins define the identity of the membrane domains. Polarized sorting of vesicles containing membrane-associated proteins into distinct membrane domains is important for maintaining the apicobasal membrane polarity in expanding membranes (Mellman and Nelson, 2008; St Johnston and Ahringer, 2010). *In vivo* studies on *Caenorhabditis elegans* have shown that sphingolipid biosynthesis is essential for maintaining the apicobasal polarity of the growing intestine and for organismal survival, suggesting that sphingolipids on the plasma membrane and the sorted vesicle membranes determine apical membrane identity and regulate apical sorting (Seamen et al., 2009; Zhang et al., 2011). However, the molecular mechanisms for maintaining the membrane polarity and preserving the membrane identities are still not clear.

The Hpo pathway in *C. elegans*

Several components of the Hpo pathway and genetic interactions between them are conserved in the nematode *C. elegans* (Cai et al., 2009; Iwasa et al., 2013; Kang et al., 2009); *wts-1*, *yap-1*, and *egl-44* are some examples of this (Iwasa et al., 2013). A study showed that the subcellular localization of YAP-1, the worm homolog of YAP/Yki, is regulated by WTS-1, the worm homolog of LATS/Warts, in the hypodermis. It was also shown that YAP-1 binds to EGL-44, the worm homolog of TEAD/Sd (Iwasa et al., 2013). The biological significance of the conservation of the Hpo pathway in worms is that it serves different purposes from its homologs reported in mammals and flies. The Hpo pathway in the hypodermis is reported to be involved in heat stress responses and in lengthening the health span of worms (Iwasa et al., 2013). Another study showed that loss of WTS-1 activity caused defects in the maintenance of apicobasal polarity in the intestine (Kang et al., 2009). It is interesting to note that the *wts-1* mutant worms initially established normal apicobasal polarity, but later began to display the gradual exocytosis-mediated mis-localization of apical proteins to the basolateral region, and ultimately died. This implies that the Hpo pathway may be involved in the maintenance of the membrane

identities in growing membranes.

Neuronal roles of the Hpo pathway

While the Hpo pathway functions in growth control are well understood, its functions in neurons are relatively unknown. It usually functions in early development of neurons including neuronal progenitor cell proliferation and survival. In the developing of the vertebrate neural tube, loss of LATS activity lead the expansion of neuronal progenitor pools in YAP and TEAD activities dependent manners (Cao et al., 2008; Fernandez et al., 2009). In *D. melanogaster*, Hpo and Wts act in dendrite tiling and maintenance of sensory neurons (Emoto et al., 2006; Parrish et al., 2007). The Worm homolog of NDR kinase which is the evolutionary conserved subclass of AGC group kinase with Wts (Pearce et al., 2010), *sax-1* is known to acts in dendrite termination of touch receptor neurons (Gallegos and Bargmann, 2004).

Purpose of this study

In this study, I wanted to define the roles of the Hpo pathway in different two

tissues of *C. elegans*, intestine and neurons. In the case of intestinal roles of the Hpo pathway, to elucidate the molecular mechanism of WTS-1-involved maintenance of cellular polarity, I tried to investigate the genes acting downstream of *wts-1* using forward genetic screening. Moreover, I also aimed to find out a transcriptional target of the Hpo pathway for maintaining cellular polarity. Also, I tried to determine worm homologs of upstream factors of LATS kinases acts in upstream of *wts-1* in this phenomenon to figure out the conserved Hpo pathway is functional in *C. elegans*.

In case of the roles of Hpo pathway in neurons, I focused on the structurally disintegrated neurons of worm lacking both the Hpo pathway and the Wnt pathway. Through various genetic approaches, I tried to figure out the molecular mechanism of this trait and to find a mechanism to restore neuronal integrity. Considering that structural disintegrity of neurons is a hallmark of aged neurons, my works will contribute to further understanding of the molecular mechanism of neuronal aging at cellular level.

Materials and Methods

Worm maintenance and used strains

Worms were maintained at 20℃ and handled as previously described (Brenner, 1974), unless noted otherwise. The Bristol strain N2 was used as the wild type. The following mutant strains were used: VC590 *wts-1(ok753)/hT2[qIs48]*, *wts-1(ok753)*; Ex[*wts-1*pro(2.7 kb)::*wts-1*::*gfp*, *sur-5*pro*::sur-5::gfp*] (Kang et al., 2009), VC590; Ex[*act-5*pro::*act-5*::*gfp*] (Kang et al., 2009), *yap-1(tm1416)*, *yap-1(snu2)*, *yap-1(snu3)*, *yap-1(snu4)*, *yap-1(snu7)*, *yap-1(snu8)*, *egl-44(n1080)*, *egl-44(snu9)*, *egl-44(snu11)*, *tat-2(tm2332)*, VC555 *nfm-1(ok754)/hT2[qIs48]*, HT1593 *unc-119(ed3)*. RB763 *cwn-1(ok546)*, VC636 *cwn-2(ok895)*, SK4005 *zdIs5* [*mec-4*pro*::*GFP + *lin-15(+)*] , CF1192 *egl-27(n170) ; muIs35* [*mec-7*pro*::*GFP + *lin-15(+)*].

Molecular biology

For the intestinal expression of YAP-1, the entire *yap-1* was cloned into pPD114.108 under either the own 4 kb promoter or the *opt-2* promoter. For *tat-2* promoter, 3 kb *tat-2* promoter was cloned into pPD117.01 vector. For the *wts-1* RNA*i* construct, the *wts-1* cDNA (bases 350-1550) was cloned into the L4440 vector (Kang et al., 2009). For touch

neuron-specific rescue of YAP-1, GFP fused at its N-terminus YAP-1 was cloned under *mec-17* promoter or *mec-4* promoter using Multisite Gateway Cloning kit (Invitrogen, US). To make constitutive active forms of YAP-1, phosphorylation dead form mutation in the coding region of YAP-1(S194A) was produced by a site-directed mutagenesis or NLS from SV40 vector was tagged to YAP-1. To clone a dominant negative mutation form of POP-1, the N-terminus deleted POP-1 was cloned into *mec-4* promoter added the pPD114.108 vector. To visualize dopaminergic, GABAergic and cholinergic neurons of worms, *dat-1* promoter, *unc-47* promoter, and *cho-1* promoter respectively, were fused to GFP using a standard fusion PCR methods. For the *unc-54* RNA*i* construct, 2000 bps from 6^{th} exon region was cloned into the L4440 vector.

Transgenic lines

For the intestinal YAP-1 expression, I introduced *opt-2*pro::YAP-1::GFP constructs with UNC-119 wild-type copies to a *unc-119(ed3)* background using bombardment. Then I isolated the worms in which the uncoordinated phenotype was suppressed. Since the penetrance of transgenes was not 100%, transgenes seemed to be transferred as

extrachromosomal arrays. All other plasmids were injected into worms at 50ng/μl with 50ng/μl of pRF4 marker, unless noted otherwise. For touch neuron-specific rescue of YAP-1 in *wts-1; cwn-1; yap-1* triple mutants, 50ng/μl of *mec-4*pro::GFP::YAP-1 was injected to worms with 50ng/μl of *myo-2*pro::mCherry as transgenic marker.

EMS mutagenesis and mapping of responsible genes

To isolate suppressors of *wts-1(ok753)* lethality, *wts-1(ok753)*; Ex[*wts-1*pro::*wts-1*::*gfp*, *sur-5*pro::*sur-5*::*gfp*] animals were treated with 50 mM EMS and approximately 10,000 worms of F1 generation were plated. Suppressor mutations were identified by the absence of GFP-SUR-5 signal. A total of 14 independent suppressor lines were maintained. Using SNP mapping and manual sequencing of the YAP-1, EGL-44 coding regions, we found that 5 of them had mutations in the YAP-1 coding region and 2 of them, in the EGL-44 gene.

Analysis of L1 viability

To measure the L1 viability of worms, I transferred 20 day1 gravid adult worms to a

Nematode Growth Medium (NGM) agar plate and removed them after 2-3 h leaving laid eggs. I counted the number of total embryos and after one day, checked the number of unhatched embryos. Two days later, I checked the number of adults. The L1 viability was calculated as the ratio of the number of adults to the total number of hatched L1 individuals (the # of total embryos – the # of unhatched embryos). For each genotype, analyses were repeated at least three times.

Analysis of the cellular polarity

We monitored the apical protein sorting using the GFP-ACT-5 expression. For each genotype, 20 day1 adults were transferred to a NGM plates and removed after 12 h. Three days later, the distribution of GFP-ACT-5 in the worms at L4 stage were observed using a fluorescence microscopy (Axioplan2, Carl Zeiss, Inc.,). For isolating *wts-1* homozygous mutants, we isolated L1 worms that did not display a pharyngeal GFP signal since VC590 *wts-1(ok753)/hT2[qIs48]* was maintained as the heterozygote. Three days later, L1 arrested *wts-1* homozygote mutant worms were used for analysis of the cellular polarity.

Gene expression comparison by microarray and data analysis

To collect embryos of N2 and *yap-1(snu8),* gravid adults from 10 plates of 10cm NGM lite for each genotype were bleached. Total RNAs were extracted from 3 biological replicates by the freezing-thawing method. The isolated RNAs were qualified and used as templates for cDNA synthesis in the Genome Research Facility of the Seoul National University using an Affymetrix chip (Seolin Bio, Seoul, Korea). The chip data were analyzed using the Microarray Suite version 5.0 (MAS 5.0) with global scaling performed as the normalization method using Genplex ver.3.0 (istech.inc). Significant genes were obtained by fold-change calculating and Welch's T-test (P-value $\leq$ 0.05) using Volcano Plot and filtering A (absent) by detection call.

Quantitative real time PCR

Primers used for the validation of candidate genes:

ORF name	Gene name	Forward primer	Reverse primer
F32A7.6	*aex-5*	5'- GTTTGAGGCTCAGTGGAAGC -3'	5' - GCTTCCCGGATGTAAAGTGA -3'
F15E11.13	*pud-1.1*	5'- ATGGGATGCGGATAAGTCTG -3'	5' - CCGATTTGGTGACCTTTGTT -3'
F37A4.3		5'- CAATTCTCCGGGATTTTCAC -3'	5' - TTTCCGGCAAATACCTAACG -3'
H22K11.4	*sgca-1*	5'- TCGAACGTCGAAATCATTCA -3'	5' - TGTGACCGGTGTGCCTATTA -3'

Y4C6B.3		5’- GTGAGCGGAGTGATCTGTGA -3’	5’ - TTTCCAAGCTCTTTGGCACT -3’
F28H6.1	*akt-2*	5’- CTTTTGCGGAACACCAGAAT -3’	5’ - TTCGAAGAGTTTGCCGTTCT -3’
F58G11.1	*letm-1*	5’- CTAGATGGTGCATTCGCTGA -3’	5’ - CAAATCAACGCTGTTCTCCA -3’
F54F2.7		5’- GGATTTTGGAACGACGAAGA -3’	5’ - GAACACCTGCTCTCACGACA -3’
C16A11.9	*fbxc-43*	5’- ATCGGATAACCCCCTAATCG -3’	5’ - TATTCCCGGTCTTGTTGGAG -3’
C52E12.4	*ist-6*	5’- AAGGTGGAGGACACAATTCG -3’	5’ - GTTGTGCCGAGTAACGGAAT -3’
F11C1.1		5’- ACACCAACCCGAATGATGTT -3’	5’ - CACTCCATAAACGCCATCAA -3’
H13N06.2		5’- TGGGAAATCGAAGAAACCTG -3’	5’ - TTTTGCCATTTGGTTCTTCC -3’
K10B2.2	*ctsa-1*	5’- AGCGACCAAGTTGGAAAGAA -3’	5’ - GCCTCGTTCACTTTCTCCTG -3’
Y39B6A.33		5’- CCGAAATACGGAAAAGACGA -3’	5’ - ATGTGAATCCTGCTCCTTGG -3’
H06H21.10	*tat-2*	5’- CTGTTTTGGCAATGGGATCT -3’	5’ - TGCGTTGTAAAATGCACCAT -3’
ZC434.3		5’- ATGTTGGAACCGACCCATTA -3’	5’ - AATCAAATCTCCAGCCATGC -3’
T19D12.7	*oig-8*	5’- TCCGCTCGTTTCAGAAAGTT -3’	5’ - TCCAGGCATTTCATCAACAA -3’
F56C9.7		5’- TTGGCAATTGGAACGTGTAA -3’	5’ - TTGAACGAATTGCTGACGAG -3’
R193.2		5’- AGTCGGTCCATCTTCCACAC -3’	5’ - TGCCAAATCTGCGTCAGTAG -3’

For all cases, the expression level of *act-1/3* gene were used as a control. Forward: 5’-ACG CCA ACA CTG TTC TTT CC-3’ Reverse: 5’-GAT GAT CTT GAT CTT CAT GGT TGA-3’

RNA*i* feeding experiments

For RNA*i* of the Hpo pathway components, we used the constructs from the J. Ahringer libraries. RNA*i* feeding experiments were done by standard methods. 4-6 L4 worms were transferred to plates with bacteria expressing RNA*i* constructs, and subcellular localization of YAP-1 was observed in progeny worms at L1 stage. For *sptl-1* RNA*i*, wild-type N2 and *yap-1(tm1416)* embryos were transferred to either the control plates or

sptl-1i plates and two days later, 20 L4 worms for each genotype (P0) were transferred to new RNA*i* plates individually. Survival rate of P0 and their progenis (F1) were scored. Three times repeated. For *unc* gene RNA*i* experiments, 4-6 *wts-1; cwn-1* mutants were transferred to RNA*i* plates, and the numbers of ectopic branches were measured at L4 stage of F1 generations.

Microscopy

Fluorescence images (Fig 4, 15, 17, 19, 21, 23, 26, 28, 30, 32, 34B) were acquired using the confocal microscope (ZEISS LSM700, Carl Zeiss, Inc) and other images (Fig 3, 5, 11B, 31, 33, 36, 38) were acquired from a microscope (Axioplan2, Carl Zeiss, Inc).

Results

Part I. The NFM-1-WTS-1-YAP-1 pathway in *C. elegans*

Identification of *yap-1* and *egl-44* as suppressors of *wts-1*

Worms that lacked WTS-1 activity displayed early larval lethality because of defects in cellular polarity in their intestines (Kang et al., 2009). Although they established normal cellular polarity at the beginning, they failed to maintain it and gradually displayed basolateral and vesicular distribution of apical proteins.

To elucidate the molecular mechanism by which cellular polarity is maintained in the expanding membrane, I performed a forward genetic screening to identify downstream factors of WTS-1. I treated mutagen Ethyl Methane Sulfonate (EMS) to the *wts-1* mutants expressing wild-type copies of WTS-1 fused with GFP and SUR-5 marker as transgenes. In the F2 generation, I isolated worms that survived without transgene expression (Fig. 1A). After 10,000 F1 screenings, 14 independent suppressor lines were obtained and maintained. Using Single-Nucleotide Polymorphism mapping and manual sequencing, I found that 5 of them had mutations in *yap-1*, while 2 of them had mutations in *egl-44* (Fig. 1B, C). *yap-1* and *egl-44* are *C. elegans* homologs of YAP/Yki and

TEAD/Sd, respectively, which are highly conserved downstream factors of LATS/Warts kinase (Iwasa et al., 2013). Among the 5 alleles of the mutant *yap-1*, *yap-1(snu4)* and *yap-1(snu7)*, which produced truncated YAP-1 proteins containing a WW domain, displayed dominant effects (Fig. 1B). The WW domain of YAP is a well-known protein motif, which binds the PPxY motif found in several components of the Hpo pathway, including LATS kinase. These proteins bind and inactivate YAP activity both in phosphorylation-dependent (Huang et al., 2005) and -independent manners (Oh et al., 2009). In my suppressor lines *snu4* and *snu7*, which lack WTS-1, the imperfect YAP-1 containing the WW domain might compete with the intact YAP-1 for binding with the PPxY motif or other unknown binding factors and display dominant effects.

Mutations of *yap-1* and *egl-44* suppress *wts-1* mutant phenotypes

yap-1 and *egl-44* mutations can suppress the early larval arrest phenotype of *wts-1* mutants. In addition to the 5 alleles that were obtained from our screen, a putative null mutation of *yap-1(tm1416)* also allowed a *wts-1* mutant to develop to a post-larval stage (Fig. 2). In the case of *egl-44*, the conventional mutant *egl-44(n1080)* failed to

suppress early larval lethality in *wts-1(ok753)* (data are not shown), and I excluded this allele from our analysis (see Discussion). *yap-1* and *egl-44* mutations that suppress the lethality also suppressed the polarity defects of *wts-1* mutants. Double mutants with *wts-1* and each *yap-1* or *egl-44* mutant alleles displayed normal distribution of apical protein ACT-5 on the luminal membrane of the intestine (Fig. 3). Although *wts-1; yap-1(snu2)* mutants showed abnormal distribution of ACT-5 in the basolateral region, they were able to overcome lethality (Fig. 3, white arrow). These data suggest that YAP-1 and EGL-44 activity are required to induce polarity defects and eventual death in *wts-1* mutants. Thus, proper regulation of YAP-1 and EGL-44 by WTS-1 during development is essential for the polarized sorting of newly synthesized proteins and for maintaining cellular polarity in expanding membrane.

WTS-1 regulates subcellular localization of YAP-1 in intestine

During development, YAP activity is tightly regulated by the upstream components of the Hpo pathway, whereas TEAD is constitutively localized in nucleus (Vassilev et al., 2001). Activated LATS kinase phosphorylates YAP and inhibits its

function as a transcriptional co-activator in the nucleus. Phosphorylated YAP is sequestered in the cytoplasm via an interaction with the 14-3-3 complex (Vassilev et al., 2001; Zhao et al., 2007) or undergoes phosphodegron-mediated degradation (Zhao et al., 2010). Loss of LATS kinase activity induces nuclear accumulation of YAP and abrogates the transcriptional regulation of target genes (Hao et al., 2008). In *C. elegans*, YAP-1 is expressed in various epithelial tissues including hypodermis and intestine and it is localized in the nuclei of hypodermal cells at the beginning of the ventral enclosure. After this, YAP-1 is sequestered in hypodermal cytoplasm throughout the larval stages in a WTS-1 -dependent manner (Iwasa et al., 2013). EGL-44 is known to be expressed more widely and is observed in the nuclei in various sites including intestine, hypodermis, and neuronal cells throughout development (Wu et al., 2001). This is consistent with the regulatory modalities of TEAD/Sd in other organisms.

For the maintenance of intestinal cellular polarity, WTS-1 acts in a cell-autonomous manner. Only the expression of WTS-1 in intestine, not in hypodermis, was shown to prevent larval lethality of *wts-1* mutants (Kang et al., 2009). To investigate the subcellular localization of YAP-1 and its regulatory mechanisms in the intestine, I

expressed GFP-fused YAP-1 in intestinal cells using the intestine-specific promoter *opt-2*. During development, intestinal GFP-fused YAP-1 was found to be sequestered in cytoplasm throughout the rest of the development (Fig. 4). Only late embryos and just-hatched L1 worms partially shows YAP-1 localizations in the nucleus and luminal membrane (Fig. 4). Knockdown of WTS-1 activity by RNA*i* led to accumulation of YAP-1 in the nuclei and luminal membranes of intestinal cells in the larval stages (Fig. 5). It suggested that WTS-1 is also involved in the regulation of the subcellular localization of YAP-1 in the intestine. Although wild-type N2 worms fed *wts-1* RNA*i* did not show L1 lethality, either *rrf-3* mutants which are highly sensitive to RNA*i* or transgenic worms overexpressing YAP-1 displayed L1 lethality when they fed *wts-1* RNA*i* (data are not shown).

TAT-2 is a transcriptional target of YAP-1 and EGL-44

Our genetic data suggested that the constitutive localization of YAP-1 in the intestinal nuclei of *wts-1* mutants leads to cellular polarity defects and organismal lethality in an EGL-44-dependent manner. This suggested that the misregulated target

genes of YAP-1 and EGL-44 are responsible for the polarity defects and the eventual lethality of *wts-1* mutants. In other organisms, YAP/Yki and TEAD/Sd complexes in the nucleus has been shown to regulate the expression of several genes like *cyclin E, diap,* and *bantam,* which promote organ growth (Harvey et al., 2003; Hu et al., 2004; Wei et al., 2007).

To identify target genes of the Hpo pathway for cellular polarity maintenance, I compared the expression levels of all the genes of *yap-1(snu8)* mutants to those of wild - type worms using a microarray experiment. Due to the nuclear localization of endogenous YAP-1 being limited to embryos and very early L1 stages (Fig. 3) (Iwasa et al., 2013), I extracted mRNA from eggs. I found that 29 genes were significantly downregulated and 51 were upregulated in the absence of YAP-1 activity (Table. 1). Since TEAD/Sd is usually involved in YAP/Yki-mediated gene inductions (Lin et al., 2000), I focused on the genes that were downregulated in *yap-1(snu8)*. To select candidates for the Hpo pathway target genes, I measured the expression levels of these genes in the different mutant alleles of *yap-1(tm1416), egl-44(snu9),* and *egl-44(snu11)*. In *yap-1(tm1416),* 14 genes out of the top-ranked 20 genes including *tat-2,* were decreased (Fig. 6 and Fig. 8). Among

them, 8 genes including *tat-2* consistently downregulated in *egl-44* mutants (Fig. 7 and Fig. 8).

The *tat-2* mutant was isolated from the genetic screening for the suppressors of sphingolipid deficiency-mediated larval death (Seamen et al., 2009). *sptl-1* encodes a putative serine palmitoyltransferase, and its activity is required for sphingolipid synthesis (Zhang et al., 2011). Knockdown of *sptl-1* by RNA*i* caused defects in polarized protein sorting in the growing intestine, which eventually led to the early larval death of progenies including the death of parents (Seamen et al., 2009; Zhang et al., 2011). Introduction of *tat-2* mutation into this sphingolipid-deficient worm suppresses L1 lethality of progenies without restoration of lipid synthesis and worm-bag mediated death of parents. Interestingly, I found that the loss of YAP-1 also suppressed the lethality of sphingolipid-deficient worms (Fig. 9). Survival rates of *yap-1(tm1416)* fed with *sptl-1* RNA*i* were relatively lower than those of *tat-2(tm2332)*. This seemed to be due to the lower larval survival rate of *yap-1(tm1416)* itself (Fig. 9, Fig. 2A). These results indicated that TAT-2 was a strong candidate for a YAP-1 and EGL-44 target.

tat-2 alone suppresses polarity defects and larval lethality of *wts-1* mutants

I speculated that ectopically increased TAT-2 was responsible for the disruption of the membrane polarity and early larval lethality of *wts-1* mutants. *tat-2* expression levels were significantly increased in the absence of *wts-1* (Fig. 10). To test our hypothesis that larval lethality of *wts-1* is due to the ectopic expression of *tat-2*, I introduced a *tat-2* mutation into *wts-1* mutants. Surprisingly, I found that *tat-2* mutation alone suppressed the larval lethality of *wts-1* mutants. About 20% of *wts-1(ok753); tat-2(tm2332)* progeny survived and developed into adults (Fig. 11A). Also these double mutants displayed normal distribution of apical proteins in their apical lumens (Fig. 11B). These data suggest that *tat-2* is a target gene of the Hpo pathway solely responsible for the maintenance of cellular polarity in *C. elegans* intestine and that transcriptional regulation of *tat-2* is essential for maintaining the structural integrity and for organismal survival.

NFM-1, the Ce_NF2/Merlin, is also involved in the polarity maintenance

Merlin/NF2 is known to act upstream of the core kinase components of Hpo

pathway in a cooperative manner with Expanded and Kibra (Baumgartner et al., 2010; Genevet et al., 2010; Hamaratoglu et al., 2006; Yu et al., 2010; Zhang et al., 2010). Merlin, Expanded, and Kibra colocalize at the apical membrane of epithelial cells (Boedigheimer et al., 1997; Yu et al., 2010) and have been suggested to recruit the Hpo pathway kinase to the apical membrane for activation. *C. elegans* has one homolog of NF2/Merlin, NFM-1 (Gobel et al., 2004). NFM-1 shares some characteristics of the Merlin/NF2, including the FERM domain at the N-terminus following the alpha helix domain (Fig. 12A). NFM-1 was expressed in various epithelial tissues including intestine and hypodermis as well as in gonad sheath cells; it was also found to be subcellularly localized in both apical and basolateral membranes of the intestine (Kang, 2010).

Remarkably, *nfm-1(ok754),* similar to *wts-1(ok753),* displayed a gradual conversion of apicobasal polarity and became lethal at the first larval stage (Fig. 12A) Introduction of a *yap-1* mutation led to post-L1 development in *nfm-1* mutants (Fig 12B). About 60% of *nfm-1(ok754); yap-1(tm1416)* double mutants were found to develop until the late L3 stage. However, these mutants failed to develop to the adult stage because of defects in the germline development (Kang, 2010). Consistent with these findings,

extrachromosomal expression of NFM-1 in *nfm-1* mutants allowed only post-L1 development. Rescued worms developed until the late L3 stages and then died (Kang, 2010). This suggested that other unknown factors act downstream of *nfm-1* during germline development. Nevertheless, these genetic data show that NFM-1 the well conserved upstream of the Hpo pathway might act upstream of WTS-1 to regulate YAP-1 and that the conserved NFM-1-WTS-1-YAP-1-EGL-44 pathway functions in maintaining apicobasal polarity in *C. elegans* intestine.

CST-1 and CST-2 may act redundantly upstream of YAP-1

The highly-conserved MST/Hpo kinase functions as one of the core Hpo pathway components along with LATS/Warts and YAP/Yki. Here is still some controversy regarding the question of whether the Hpo pathway is conserved in *C. elegans* (Yang and Hata, 2013). As only WTS-1, among all the worm homologs of the Hpo pathway components, was known to control YAP-1 localization in the hypodermis, only LATS kinase, YAP, and TEAD were thought to be conserved as signaling components in *C. elegans* (Iwasa et al., 2013; Yang and Hata, 2013). Consistent with the

results of the hypodermis, RNA*i* against each worm homolog of the Hpo pathway components failed to induce nuclear accumulation of YAP-1 in intestine (Fig. 13B). However, knockdown of *cst-1* and *cst-2*, the worm homologs of Mst/Hpo kinase, triggered partial nuclear localization of YAP-1 in intestine. Therefore, CST-1 and CST-2 might redundantly act as the Hpo kinase upstream of WTS-1 as they also share 99% sequence similarity (Lehtinen et al., 2006).

Part II. The roles of the Hpo pathway in *C. elegans* neurons

yap-1 and *egl-44* mutants display polarity defects in ALM

From the phenotype analysis of *yap-1* and *egl-44*, I found that they have defects in ALM development. Six mechano-sensory neurons (2 ALM, 2 PLM, AVM, PVM) govern aversive forward and backword movement in response to body touches. ALM and PLM neurons cover anterior parts and posterior parts of the whole body, respectively, sense gentle mechanical stimuli and transmit signals to command neurons to trigger aversive movement (Chalfie et al., 1985). Both ALM and PLM cell bodies migrate

posteriorly and extend their processes to anterior from their cell bodies. Due to their developemental characteristic along anterior-posterior body axis, ALM and PLM neurons have been used as developmental models along Anterior-Posterior body axis. Loss of *yap-1* or *egl-44* causes various developmental defects in ALM neuronns including bipolar outgrowth, premature stop of cell bodies, neurite guidance abnormalities and loss of GFP driven by *mec-4* promoter in ALM (Fig. 15 lower panel). Among these, since bipolar outgrowth of ALM was the most prominent phenotype of mutants, I focused on the roles of YAP-1 and EGL-44 in asymmetric development of ALM neurons. Various mutant alleles of *yap-1* and *egl-44* including putative null mutation of *yap-1(tm1416)* lost their asymmetry and ectopically extended their processes posteriorly (Fig. 16A, B).

yap-1 and _egl-44_ act in the polarized ALM development in cell autonomously

Six TRN (touch receptor neuron)s including ALM terminate development during embryogenesis. To define whether *yap-1* and *egl-44* are required in development or in the maintenance of ALM asymmetry, I observed ALM neurons in just hatched L1

worms which lack *yap-1* or *egl-44* activities. Both *yap-1* and *egl-44* mutant L1 had similar frequencies of bipolar outgrowth of ALM neurons with those of L4 worms (Fig. 17). When YAP-1 activities were rescued in touch receptor neurons specifically, bipolar outgrowth phenotype of *yap-1(tm1416)* was significantly decreased (Fig. 18). Moreover, subcellular localization of YAP-1 in ALM neurons was spatio-temporary regulated. GFP-fused YAP-1 under the control of *mec-4* promoter, localized in the ALM nuclei only in embryos. From L1 stages, YAP-1 was always sequestered in the cytoplasm of ALM (Fig. 19). These spatiotemporal regulation modalities of YAP-1 in ALM are consistent to those in intestine. These data suggested that during embryogenesis, YAP-1 and EGL-44 might act asymmetric development of ALM neurons in cell autonomous manners.

YAP-1 may act in same genetic pathway with the Wnt pathway

In the past decades, many polarity determinants of neurons were identified. Slit/netrin signaling usually regulates neuronal development along Dorsal-Ventral Axis (Hao et al., 2001; Killeen and Sybingco, 2008) and the highly conserved Wnt pathway has been known to orient neurite outgrowth along A-P axis (Killeen and Sybingco, 2008;

Prasad and Clark, 2006). I tried to figure out YAP-1 and EGL-44 acts in same genetic pathway with Wnt, the most famous regulator of A-P polarity. *C. elegans* genome contains five Wnt genes (*mom-2, lin-44, cwn-1, cwn-2, and elg-20*) and four frizzled genes, Wnt receptors (*mom-5. lin-17, mig-1, cfz-2*) (Korswagen, 2002). Among 5 genes coding Wnt ligands, loss of *cwn-1* or *cwn-2* was known to break the asymmetry of ALM neurons (Prasad and Clark, 2006). I found that introduction of *yap-1* mutation into either *cwn-1* or *cwn-2* mutant did not lead to the further increase of polarity defects of ALM (Fig. 20). It said that YAP-1 may acts in same genetic pathway with Wnt in asymmetric development of ALM. I tried to make a triple mutant, *cwn-1; cwn-2; yap-1*, however failed to obtain it likely due to embryonic lethality of triple mutants.

Ectopic neuronal branching in *wts-1; cwn-1* double mutants

Among various mutants I generated, *wts-1; cwn-1* double mutants had a interesting phenotype in touch receptor neurons. They had ectopic neuronal branches on processes of ALM and PLM (Fig. 21). Moreover, they also displayed bipolar outgrowth of ALM neurons which was similar to those of *yap-1* or *egl-44* mutants (white arrow in

Fig. 21). Ectopic neuronal branching events were observed only in *wts-1; cwn-1* double mutants. *wts-1; cwn-2* double mutant had intact neurnal processes of touch recptor neurons. Since loss of WTS-1 activity causes organismal lethality, the lethality of *wts-1* was rescued by the intestinal expression of wild type copies of WTS-1. Therefore, I could exclude the possibilities that WTS-1 functions in the intestine in this phenomenon.

wts-1; cwn-1 **has defects in the maintenance of the neuronal integrity**

To figured out *wts-1; cwn-1* mutants had defects in the development of TRNs or in the maintenance of TRNs structure, I observed TRN morphologies of *wts-1; cwn-1* embryos. Both in wild type and mutant embryos, TRNs terminated the development and displayed mature morphological features (Fig. 23). Moreover, I found that *wts-1; cwn-1* mutants had intact, undamaged neuronal processes of TRNs (Fig. 23). Moreover, the frequencies of ectopic neuronal branching on TRNs were gradually increased as worms grow and get older (Fig. 24). *wts-1; cwn-1* mutants did not show ectopic neuronal branches in embryonic stage and L1 stage, however, almost of them displayed disintegrated neurons from 5 days in their adulthoods. These results showed that *wts-1;*

cwn-1 mutants had defects in the maintenance of structural integrity of TRNs, not in the development of TRNs. In case of bipolar outgrowth of TRNs, about 20% of ALMs of *wts-1; cwn-1* displayed bipolar defects and the penetrance of defects was gradually increased, too (Fig. 24). Considering that *cwn-1* itself acts in the polarized development of ALM (Fig 20) (Prasad and Clark, 2006), defects at L1 stage was likely due to the absence of *cwn-1*.

And then, to define whether *wts-1* and *cwn-1* acts in the structural maintenance of neurons generally or TRNs specifically, I scored the morphologies of other types of neurons in *wts-1; cwn-1*. In *wts-1; cwn-1* mutants, dopaminergic, GABAergic and cholinergic neurons maintained intact processes at L4 stage (Fig. 26). Especially, cholinergic neuron, ALN which extends their process in association with ALM neurons, maintained their structural integrity (Fig. 26 right panel). Thus, I concluded that structural dis-integrity of *wts-1; cwn-1* mutant was specific to TRNs.

As I mention earlier, TRNs including ALM, PLM govern aversive movement of worms in response to body touch. To know that structural dis-integrity of *wts-1; cwn-1* affects touch responses of worms or not, I measured touch responses of *wts-1; cwn-1*

mutants. I measured the number of responses per total 10 touches of individual worm and 30 worms of each strains were tested for one experiment. *wts-1; cwn-1* mutants had significantly decreased responses to gentle body touches (Fig. 27).

yap-1 and *egl-44* suppress structural dis-integrity of *wts-1; cwn-1* mutants

To know *yap-1* acts in the downstream of *wts-1* and *cwn-1* in this phenomenon, I introduced *yap-1* mutation into *wts-1; cwn-1* mutants, and found that *yap-1* mutation completely suppressed neuronal branching (Fig. 28, right panels) whereas it leaves 30 % of ALM neurons with bipolar outgrowth (white arrow in Fig. 28, quantification data was not show). I thought that the absence of *yap-1* was responsible for these polarity defects. Moreover, introduction of *yap-1* mutations also partially suppressed touch insensitivities of *wts-1; cwn-1* mutants (Fig. 29A, B). Therefore, it suggested that mutation of *yap-1* suppresse not only the structural dis-integrity of *wts-1; cwn-1*, but also the functional defect of TRNs. Introduction of *egl-44* mutation was also sufficient to suppress ectopic neuronal branches and failed to suppress polarity defects of ALM (Fig. 30, right panels).

Regulation of YAP-1 in TRNs is required to maintain neuronal integrity

I wanted to know the action site of YAP-1 and EGL-44 in maintenance of neuronal integrity. To determine YAP-1 acts in cell autonomous manner or not, I injected the plasmid contains YAP-1 wild type copies under the control of *mec-4* promoter into *wts-1; cwn-1; yap-1* triple mutants. Touch neuron specific rescue of YAP-1 was sufficient to de-suppress ectopic neuronal branches (Fig. 31). Not all transgenic worms expressing TRN specific YAP-1 displayed branches, about 40% of transgenic worms had ectopic branches on their TRNs. It said that *yap-1* and possibly *egl-44* act in cell autonomous manner to induce structural dis-integrity of TRNs and proper regulation of them is important to maintain neuronal structural integrity.

YAP-1 may act in parallel with the Wnt pathway

Next, I asked whether *yap-1* acts in downstream both of *wts-1* and *cwn-1*. If so, expression of constitutively active form of YAP-1 would be sufficient to induce ectopic branches. YAP-1 is known to be inhibited by phosphorylation-mediated sequestering it

in cytoplasm (Fig 5) (Iwasa et al., 2013). To make YAP-1 constitutively active, we took two strategies. I introduced phosphorylation dead mutation in *yap-1*(S104A) or fused NLS to YAP-1. Neither the phosphorylation dead form of YAP-1 nor NLS fused YAP-1 was not trigger ectopic branches in TRNs (Fig. 32, white columns). Only introduction of each of them into *cwn-1* mutant background partially induced the structural dis-integrity of TRNs (Fig. 32 black columns). Therefore, WTS-1-YAP-1 and CWN-1 might act in parallel pathway to maintain structural integrity of TRNs.

The canonical Wnt pathway in TRNs does not affect structural integrity

To verify downstream events of *cwn-1*, the Wnt ligand, I abrogated the canonical Wnt pathway only in TRNs by expressing dominant negative form of POP-1, the worm homolog of Tcf which is the most downstream factor of the canonical Wnt pathway. N-terminal deleted TCF/POP-1 is known to have a dominant negative effect, as it remains to bind corepressor (Cavallo et al., 1998; Korswagen et al., 2000; Roose et al., 1998). However, introduction of touch neuron specific DN form of POP-1 into *wts-1* mutant did not result in induction of ectopic neuronal processes (Fig. 33). This showed

that the canonical Wnt pathway did not function in the maintenance of TRNs in cell autonomously. I assumed that the non-canonical Wnt pathway in TRNs acts in this phenomenon or the canonical pathway acts in differential tissue to regulate TRNs integrity.

Decreased movement suppresses the induction of ectopic branches

Then, I asked the reasons why ectopic neuronal branching occur in *wts-1; cwn-1* mutants. I hypothesized that the absence of *wts-1* and *cwn-1* affected the microtubule stability, and physical stresses which were triggered by organismal movement induce abnormal branching or breakages on the neuronal processes. To test this hypothesis, I made worms move less by knock down several muscle machinery genes. Feeding RNA*i* against muscle machinery genes induced un-coordinated movement of worms (Fig. 34A). In compare to worms fed empty vector, *wts-1; cwn-1* mutants fed *unc-54* RNA*i* were move less and some of them were immobilized. *wts-1; cwn-1* mutants fed *unc-54* RNA*i* showed the significantly decreased numbers of ectopic branches both in ALM and PLM (Fig. 34B). Knock down of other *unc* genes which also encode muscle machinery showed similar effects. In every gene I tested, the

severeness of induced *unc* phenotype was correlated with the degree of reduction of ectopic branching (Fig. 35A, B).

Age-related characteristics of neurons in *wts-1; cwn-1* mutant

In the observations of *wts-1; cwn-1* mutant neurons, I found that they share many morphological characteristics with aged neurons. From *C. elegans* to mammals, aged neurons show the structural and functional decline (Bishop et al., 2010; Pan et al., 2011; Toth et al., 2012). In *C. elegans,* TRNs displayed the most prominent decline both in structure and function. In aged worms, TRNs have wavy or beaded processes, outgrowth of soma cell bodies and ectopic neuronal branches and touch responses governed by TRNs were decreased gradually as worms get older (Toth et al., 2012) (Fig. 37B). In addition to ectopic neuronal branches, TRNs of *wts-1; cwn-1* also showed wavy or beaded processes and soma outgrowth even before aging (Fig. 36).

Since *yap-1* or *egl-44* mutation restored neuronal dis-integrity of *wts-1; cwn-1*, I wanted to know that loss of YAP-1 delays normal aging of neurons. Thus, I measured functional decline of wild type, *wts-1; cwn-1* and *wts-1; cwn-1; yap-1* with age. In all

three genotypes, touch responses were gradually decreased as worms get older. *yap-1* mutation only partially restores touch insensitivity of *wts-1; cwn-1* and did not show aging delayed effects (Fig. 37A, B). Structural declines with normal aging were not affected or delayed due to the loss of YAP-1 (Fig. 38). Only soma outgrowth was significantly delayed in *yap-1* single mutant and *wts-1; cwn-1; yap-1* mutant in comparison with those in same aged wild type (Fig 38, first panel).

Discussion

The Hpo pathway in growing membrane of *C. elegans* intestine

In expanding epithelial membranes, the polarized sorting of newly synthesized proteins to distinct membrane domains is essential for the maintenance of structural integrity of the membranes and the survival of whole organism. Exocytosis is responsible for delivering these newly produced membrane proteins to their target destinations on the plasma membrane. In the developing intestine of *C. elegans*, WTS-1, the worm homolog of LATS kinase, is necessary for sorting newly produced apical proteins to the apical membrane domain (Kang et al., 2009). Loss of WTS-1 activity causes basolateral sorting of several apical proteins in an exocytosis-dependent manner, and this abrogated sorting triggers membrane disintegration and organismal death (Kang et al., 2009). In this study, I have shown that the conserved Hpo pathway maintains the membrane integrity by regulating the transcription of *tat-2*. I not only showed that the Hpo pathway is conserved in *C. elegans*, but also identified a transcriptional target of the pathway for maintaining membrane integrity. Our findings strongly suggest that homologs of *tat-2* may also be involved in maintaining membrane integrity in response to the Hpo signaling in other animals.

yap-1, egl-44 as downstream of WTS-1 in apicobasal polarity maintenance

Our genetic screens repeatedly identified mutations in *yap-1* and *egl-44* as downstream suppressors of the *wts-1* mutation in the maintenance of apicobasal polarity. YAP-1 and EGL-44 are worm homologs of YAP/Yki and TEAD/Sd, which are known downstream factors of LATS kinase. Consistently, a deletion mutation in *yap-1, tm1416*, also suppresses the phenotype of *wts-1* mutants. However, *egl-44(n1080)*, in which EGL-44-mediated neurogenesis is defective (Vassilev et al., 2001), failed to suppress the wts-1 mutants phenotype. The C-terminal region of TEAD/Sd is responsible for binding to YAP/Yki (Hao et al., 2008). Therefore, an EGL-44 with an abrogated C terminal in *egl-44(snu9)* and *egl-44(snu11)* might be more defective in binding with YAP-1 than one with a missense mutation in its 5th exon in *egl-44(n1080)* (Fig. 1C).

Activated LATS kinase is known to phosphorylate and inhibit YAP by sequestering it in the cytoplasm (Zhao et al., 2007). In organisms studied so far, the nuclear localization of YAP is restricted to the early developmental stages. Consistent with this, YAP-1 was localized in the hypodermal and intestinal nuclei at the beginning of ventral enclosure and then sequestered in the cytoplasm throughout larval stages (Fig. 4)

(Iwasa et al., 2013). Although I did not observe any significant phenotypic defects in *yap-1* or *egl-44* single mutants, possibly due to unidentified redundancy, it is possible that YAP-1 and EGL-44 function in early development by regulating their target gene expression.

Loss of WTS-1 activity led to abnormal accumulation of YAP-1 in the intestinal nuclei and the luminal membranes (Fig. 4). Given that the activity of EGL-44, the worm homolog of TEAD/Sd, is also needed for the causing polarity defects and lethality in *wts-1* mutants, it is possible that dysregulation of YAP-1 and EGL-44 target genes in the nucleus is responsible for these defects. A comparative gene expression study identified 29 genes whose expression was decreased in the absence of YAP-1. Among the candidate genes, *tat-2* was suspected to be a core target gene of YAP-1 and EGL-44 because it is known to mediate postembryonic growth (Seamen et al., 2009). Its expression was consistently decreased in both *yap-1* and *egl-44* mutants (Fig. 8) and increased in the absence of WTS-1 (Fig. 10). Sphingolipid deficiency-mediated larval lethality was suppressed in *yap-1(tm1416)* similar to what I observed in *tat-2(tm2332)*, and more importantly, a *tat-2* mutation was enough to suppress polarity defects and lethality in wts-

1 mutants (Fig. 11A, B). These data suggest that ectopically expressed TAT-2 in *wts-1* mutants triggered the polarity defect and larval death. I propose that *tat-2* is the responsible target gene of YAP-1 and EGL-44 for polarity maintenance. TEAD transcription factor binds the consensus CATTCC/T sequence and endogenous *tat-2* promoter has 2 CATTCT sequence within 2 kb from ATG, transcription start sequence. Further studies of EGL-44 binding motif on *tat-2* promoter will be needed.

TAT-2, a putative ATPase and cellular polarity

Then, what is the role of the TAT-2 in membrane integrity maintenance? Not only proteins but also lipids are differently distributed on plasma membrane of epithelial cells. Among them, glycosphingolipid and glycophosphoinositide (GPI) -anchored proteins are highly enriched in apical membrane (Fullekrug and Simons, 2004). However, the function of these polarized lipids and proteins in polarity maintenance is not well elucidated. Recently, unbiased reverse genetic screening showed that the lipid composition of the plasma membrane domain and the membranes of sorted vesicles could play a role as an apical sorting signal (Zhang et al., 2011). Knockdown of genes,

including *sptl-1*, which are involved in sphingolipid biosynthesis, triggered basolateral localization of newly made apical proteins and a gradual loss in the structural integrity of the intestine. Worms that lost their intestinal integrity could not absorb nutrients from the lumen and underwent death. *tat-2* mutations were isolated by an independent screening for suppressors of sphingolipid deficiency-mediated larval death (Seamen et al., 2009). Loss of TAT-2 allowed sphingolipid deficient worms to bypass lethality without restoration of lipid synthesis. TAT-2 is one of the 6 putative homologs of class IV P-type ATPase (*tat-1, tat-2, tat-3, tat-4, tat-5, tat-6*) (Gobel et al., 2004; Wu et al., 2001). Class IV P-type ATPases act as flippase, which translocate phospholipids vertically from extracytosolic leaflets to cytosolic leaflets, creating a lipid asymmetry within the plasma membrane (Yin et al., 2013). Among the 6 putative P-type ATPase genes, *tat-1* and *tat-5* were known to translocate phosphatidylserine from luminal leaflets to cytosolic leaflets, thus sequestering phosphatidylserine in the inner layer (Cheng et al., 1995; Gobel et al., 2004). Loss of TAT-1 and TAT-5 allowed phosphatidylserine to be exposed on the cellular surfaces and triggered ectopic cellular apoptosis and defects in exocytosis, respectively (Cheng et al., 1995; Gobel et al., 2004). Although the molecular characteristics of TAT-2

and its role as a flippase in the membrane remains unexplored, our genetic data suggest that ectopically expressed TAT-2 somehow changes membrane domain identity and abrogates polarized protein sorting in the growing intestinal cells. If TAT-2 translocates glycosphingolipids vertically within the phospholipid bilayer, loss or ectopic expression of TAT-2 may change asymmetry of glycosphingolipids within the phospholipid bilayer and thus influence apical transport. Tight regulation of TAT-2 expression by WTS-1 may allow animals to maintain apicobasal polarity of the intestinal membrane, which is essential for the survival of the organism.

Subcellular localization of YAP-1 at the membrane

Although I focused on the nuclear functions of YAP-1, subcellular localization of YAP-1 implies that YAP-1 has roles in the plasma membrane as well. In embryos, YAP-1 is localized in the membrane and the nucleus (Fig 4), and loss of WTS-1 triggered both membrane and nuclear localization of YAP-1 (Fig 5). Alternatively, membrane localization of YAP-1 could be a result of a WTS-1-independent inhibitory mechanism. It has been reported that Angiomotin, a membrane-associated upstream factor of the Hpo

pathway, inhibits YAP in two different ways. It can phosphorylate and sequentially activate the Hpo pathway or directly bind to YAP and sequester it in the membrane (Zhao et al., 2011). Further studies of upstream factors or unknown binding partners of YAP-1 that can possibly interact with the WW domain of YAP-1 will help to clarify the roles of YAP-1 in the membrane.

NFM-1 as upstream of the Hpo pathway in *C. elegans*

Recent studies of the Hpo pathway in *C. elegans* have found that YAP-1 and EGL-44 act downstream of WTS-1 in *C. elegans* hypodermis and that YAP-1 is involved in heat shock response and health span regulation (Iwasa et al., 2013). However, the conservation of the other components of the Hpo pathway is still unclear (Iwasa et al., 2013; Yang and Hata, 2013). Our observation that NFM-1, the conserved upstream factor of the Hpo pathway, is also involved in the maintenance of cellular polarity along with WTS-1 to regulate YAP-1 suggests extended evolutionary conservation of the Hpo pathway. Loss of NFM-1 caused defects in polarity similar to those in *wts-1* mutants and resulted in the suppression of early larval deaths caused by *yap-1* mutations. The core

kinase of the Hpo pathway is MST/Hpo kinase, which receives signals from upstream and phosphorylates and activates LATS/Warts kinase. Knockdown of *cst-1* or *cst-2*, the worm homologs of Hpo kinase, partially induced the nuclear localization of YAP-1 in the intestine. However, a putative null mutation in *cst-1* did not cause defects in polarity and larval death; CST-2 likely acts redundantly in *cst-1* mutants. Alternatively, NFM-1 may regulate WTS-1 directly. In mammals and drosophila, NF2/Merlin directly binds to and recruits LATS/Warts kinase to the membrane, leading to the phosphorylation and activation of LATS/Warts (Yin et al., 2013). However, MST/Hpo kinase activity is required for this NF2/Merlin-mediated regulation (Yin et al., 2013). Therefore, further studies are required to identify the factors that phosphorylate and activate WTS-1 in *C. elegans*. Nevertheless, evidence from our genetic studies demonstrates the role of the conserved Hpo pathway in maintaining the cellular polarity of expanding membranes (Fig. 15). Our study also provides a putative molecular mechanism for the maintenance of membrane domain identities.

The Hpo pathway in asymmetric development of TRNs

I found that YAP-1 and EGL-44 are required for asymmetric development of TRNs. So far, many polarity determinants of TRNs have been identified. Netrin mainly acts as a ventral guidance cue for AVM and PVM which are ventrally localized TRNs (Killeen and Sybingco, 2008). The Wnt pathway is the most well established polarity determinant along the Anterior-Posterior body axis. Wnt ligands are thought to form gradients along the A-P body axis, and mediate many polarized developmental aspects including not only asymmetric development of neurons but also early polarization of embryos (Killeen and Sybingco, 2008; Petersen and Reddien, 2009; Prasad and Clark, 2006; Silhankova and Korswagen, 2007). According to my genetic studies, *yap-1* might act in same genetic pathway with the Wnt pathway in cell autonomous manner to polarize ALM. Although intracellular events in polarized cell are relatively unknown, several GTPase and GTPase- interacting proteins including MIG-10 and CED-10 are thought to govern cytoskeleton remodeling (Quinn et al., 2008). Considering that GTPase acts as upstream regulator of YAP/Yki (Feng et al., 2014; Huang et al., 2016; Reginensi et al., 2013), it can be a link between the Wnt pathway and YAP-1, EGL-44. Alternatively,

unidentified target genes of YAP-1, EGL-44 could mediate asymmetric development of ALM with the Wnt pathway.

Ectopic neuronal branches in *wts-1; cwn-1* mutant

With genetic approaches, I found that loss of the Hpo pathway and the Wnt pathway leads TRNs-specific structural dis-integrity. Although *wts-1; cwn-1* mutant had intact neuronal processes at the beginning (Fig. 23), they gradually displayed ectopic neuronal branches and declined touch responses (Fig 24, 27). We suggested that defective microtubules in *wts-1; cwn-1* were broken because they could not withstand the physical stresses from movement. Because muscle abrogation-mediated movement loss decreased the numbers of ectopic neuronal branching of *wts-1; cwn-1* (Fig 34, 35). Alternatively, loss of WTS-1 and CWN-1 might affect mechano-sensation rather that microtubule stability. Previously, it was known that mechano-sensation defective mutants show structural dis-integrity of TRNs precociously (Pan et al., 2011). In TRNs, functional decline is not only a result but also a reason of structural loss. A comparison of TRNs of *wts-1; cwn-1* mutant with those of mechano-sensation defective mutant will answer this

question.

Both *yap-1* and *egl-44* act as downstream of *wts-1* in ectopic neuronal branches formation (Fig. 28, 30) and TRNs specific expression of YAP-1 was sufficient to de-suppress ectopic neuronal branches (Fig. 31). Considering *egl-44* also suppressed structural dis-integrity, identification of neuronal target genes of YAP-1 and EGL-44 will provide molecular mechanisms to maintain the structural integrity of neurons.

Damaged TRNs in *wts-1; cwn-1* mutant as a premature aging model

As mentioned earlier, structure and functional decline of neuron is a hallmark of aging. Moreover, it is also observed in several neurons of neurodegenerative diseases patients. Therefore, it has been studied extensively as a putative cause of disease. *wts-1; cwn-1* double mutant displayed age-related structural and functional loss of TRNs precociously. From L4 stages even before larval development terminates, 80% of *wts-1; cwn-1* worms had ectopic neuronal branching in their processes. Other types of neurons including ALN which extends process in association with ALM did not have these structural dis-integrity in *wts-1; cwn-1* (Fig. 26). There are several possible explanations

of TRNs specific neuronal dis-integrity in *wts-1; cwn-1*. First, YAP-1 and EGL-44 can function in TRNs specifically. Although I failed to observed YAP-1 expression in TRNs (data are not shown), touch receptor-specific expression of YAP-1 was sufficient to induce ectopic neuronal branching (Fig. 31). Alternatively, some features of TRNs can affects in this phenomenon. Consistent to this hypothesis, TRNs are known to have the most prominent decline both in structure and function with aging (Pan et al., 2011; Toth et al., 2012). Profound analysis of structure and transcriptome of TRNs in *wts-1; cwn-1* mutant will answer these questions. Further studies of molecular mechanism of these TRNs specific ectopic neuronal branching and screening of other suppressor will contribute further understandings of neuronal aging at a single cell level.

The Hpo pathway in normal aging of neurons

Whereas introduction of *yap-1* mutation into *wts-1; cwn-1* mutant was sufficient to suppress the precocious structural and functional decline of TRNs (Fig 38, 39), it failed to delay aging-related structural loss of TRNs. However, in my experiments, most of the known morphological characteristic of aged neurons were not increased as

worms get older. Only the frequency of soma outgrowth of ALM was gradually increased with aging, and loss of *yap-1* significantly suppressed soma outgrowth in aged worms (Fig 39). Moreover, my preliminary observation showed that YAP-1 re-enter the intestinal nucleus in aged organisms (data are not shown). Consistently, it was reported that in aged worms, hypodermal YAP-1 is also localized in the nucleus (Iwasa et al., 2013). These data imply that YAP-1 could function in normal aging of worms. To define the roles of YAP-1 in normal aging of neurons, observation of subcellular localization of YAP-1 in TRNs along aging should be followed.

As mentioned previously, the Hpo pathway is activated and inhibits nuclear localization of YAP-1 from late embryos. After then, YAP-1 was constitutively sequestered in the cytoplasm throughout development. Following two mechanisms explains the aging-related inactivation of the Hpo pathway. First, the Hpo pathway might be actively turn off in aged worms. After the organismal development and reproduction were finished, organism has relatively low pressure to maintain structural integrity both of intestine and neurons. Second, loss of structural integrity in aged worms could indirectly lead inactivation of the Hpo pathway. As mentioned, junctional proteins

functions as upstream signals of core kinase cascade of the Hpo pathway. Further studies about regulatory modalities of the Hpo pathway in aged worms will contribute understanding of post developmental roles of the Hpo pathway in *C. elegans*.

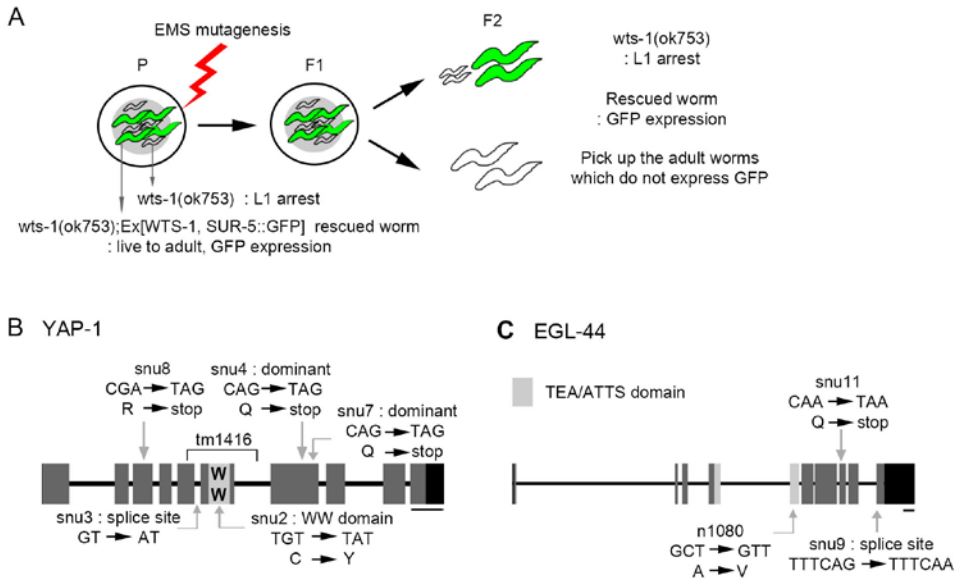

Figure 1. YAP-1 and EGL-44 are downstream targets of WTS-1. (A) A schematic diagram of the EMS mutagenesis screening to obtain *wts-1* suppressors. In the parents, extra-chromosomal WTS-1 rescues larval lethality of *wts-1(ok753)* In the F2 generation from EMS treatment, we isolated adult worms which can survive without transgenes. SUR-5-GFP was used for marking transgenes. (B) The structure of *yap-1*. The various mutant alleles of *yap-1* are shown in the figure. *snu2* is a missense mutation in the WW domain caused by a C to Y change. *snu3* disrupts the splice acceptor site of the 5th intron, resulting in a pre-mature

stop codon. *snu4* and *snu7* are dominant mutations which have pre-mature stop codons after the WW domain. *snu8* changes R to a stop codon at the N-terminus of YAP-1. *tm1416* delete from the 5th to the 6th exon including the WW domain. (C) The *egl-44* structure. Light gray box indicates the TEA/ATTS domain. *snu9* and *snu11* abrogate the C terminal region of EGL-44. *snu9* ruins the 3′ splicing site ahead of the 10th exon. *snu11* creates a premature stop codon in the 8th exon. *n1080* is a missense mutation in the TEA/ATTS domain. Scale bars are 200 bp. In collaboration with J. Kang.

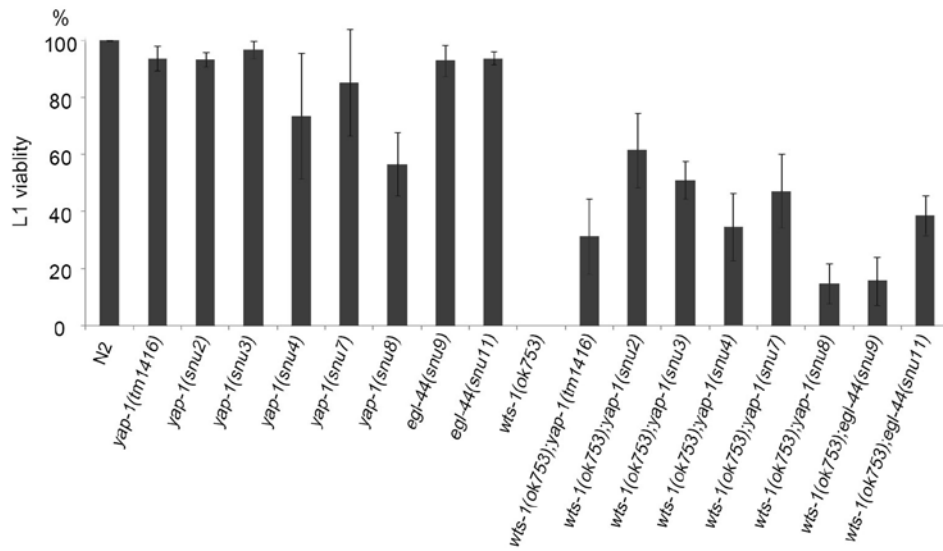

Figure 2. *yap-1* and *egl-44* suppress early larva lethality of *wts-1* mutant. Results of phenotypic analyses of *yap-1, egl-44, wts-1; yap-1, wts-1;egl-44* mutant worms. L1 viability is calculated as the ratio of the number of adult worms to total number of hatched L1 worms. Worms were grown at 20℃. In collaboration with J. Kang.

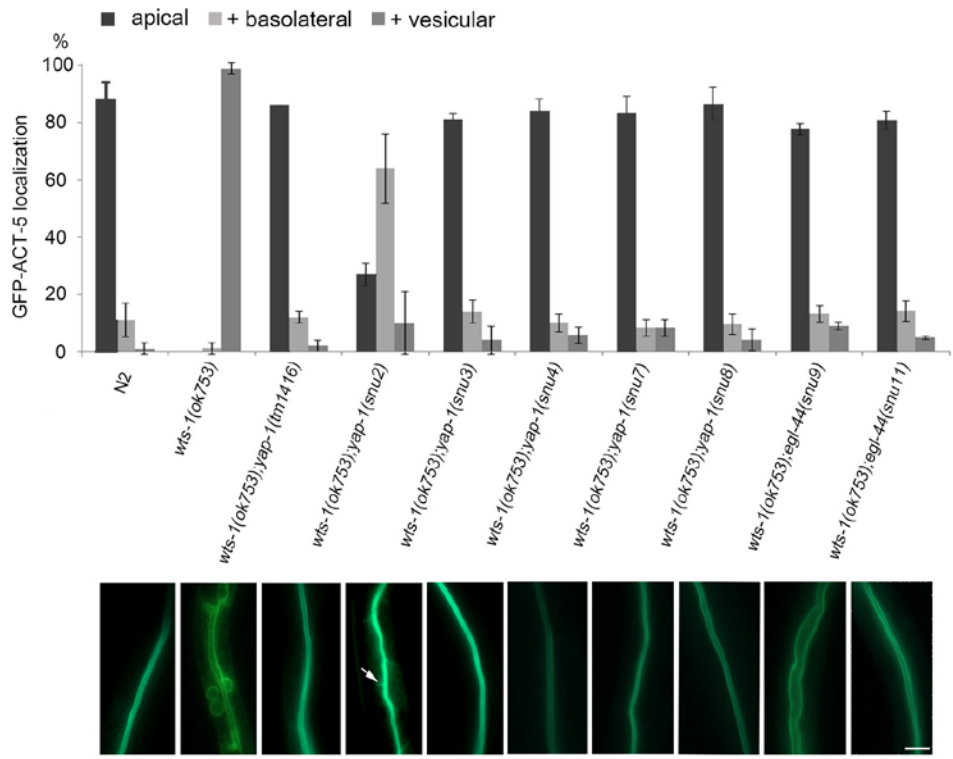

Figure 3. *yap-1* and *egl-44* suppress polarity defects in *wts-1* mutant.

GFP-ACT-5 localization in the wild type *N2*, *wts-1* mutant, and double mutant with *wts-1* and various alleles of *yap-1 or egl-44* were observed. In upper panel, '+ basolateral' indicates animals that showed apical and basolateral localization of the protein. '+ vesicle' indicates animals that had proteins localized in vesicle-like structures, in addition to the apical and basolateral sides. Two days after hatching, ACT-5 localization was observed. At the time of observation, *wts-1* mutants were

arrested at the L1 stages. The wild type, *wts-1;yap-1* and *wts-1; egl-44* worms were at the L4 stage. *snu2* only partially suppressed the polarity defects of *wts-1*. The lower panel shows the representative images of GFP-ACT-5 distribution in each genotype of the worms. Arrows indicate baso-laterally localized GFP-ACT-5. Scale bar is 10 μm. In collaboration with J. Kang.

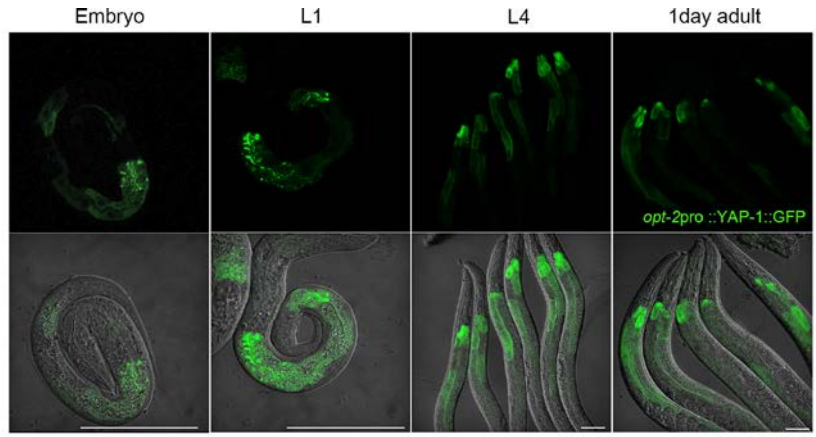

Figure 4. Subcellular localization of YAP-1 in intestine in the differential developmental stages. In the intestine, localization of YAP-1 in the nucleus and membrane was restricted to embryos and just hatched L1 worms. After the L1 stage, intestinal YAP-1 was consistently localized in the cytosol. For observation of intestinal expression of YAP-1, GFP fused YAP-1 constructs under the control of *opt-2* promoter were introduced into worms. Scale bars: 50 μm.

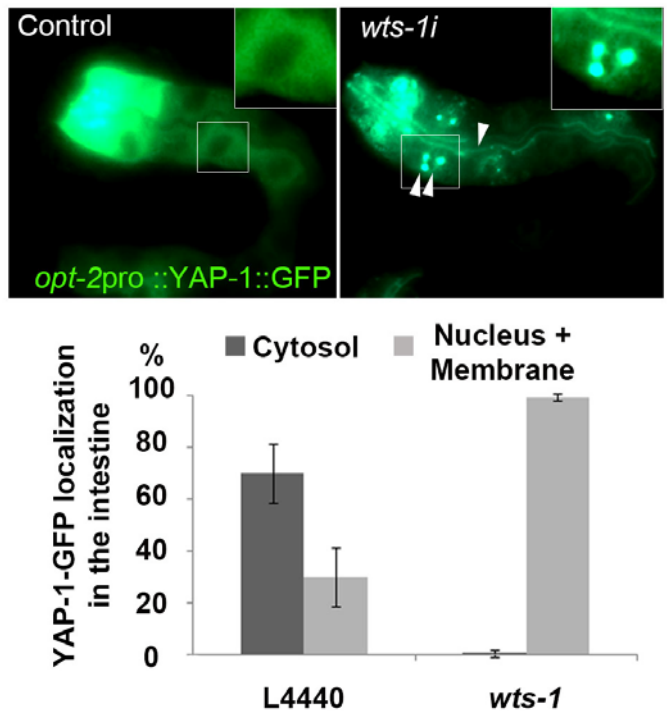

Figure 5. Regulation of YAP-1 subcellular localization by WTS-1. *wts-1* RNA*i* leads nuclear and membranous localization of YAP-1(white arrow heads). 4-6 Parental worms were transferred to plates with *E coli* expressing either empty vector or *wts-1* RNA*i* construct. In F1 generation, L1~L2 worms were used for observations (three biological replicates, 20-30 worms for each). In collaboration with J. Kang.

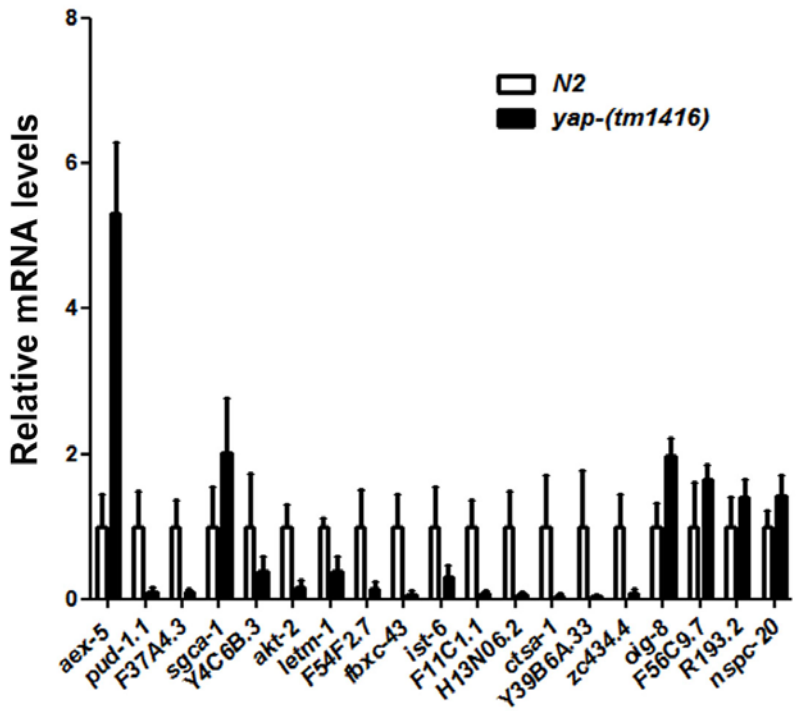

Figure 6. **Relative mRNA levels of candidate genes in *yap-1(tm1416)*.** To validate candidates for YAP-1 target genes, relative mRNA levels of each gene in other *yap-1* mutant allele *(tm1416)* were measured by quantitative real-time PCR. Total RNAs were extracted from wild type and *yap-1(tm1416)* embryos and mRNA levels of top 20 ranked genes including *tat-2* were measured (three biological replicates for each strain).

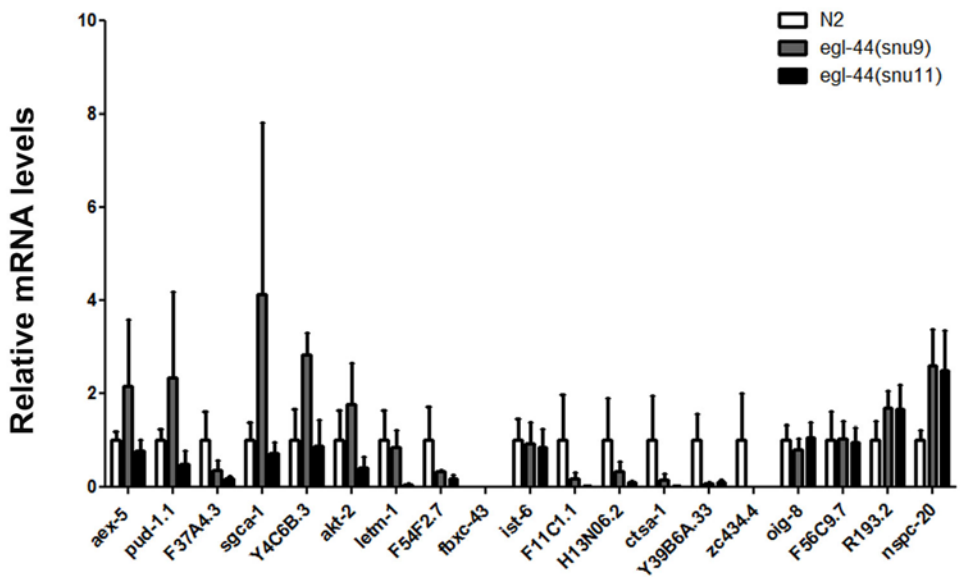

Figure 7. **Relative mRNA levels of candidate genes in *egl-44(snu9) and egl-44(snu11).*** To validate candidates for YAP-1 target genes, relative mRNA levels of each gene in *egl-44(snu9)* and *egl-44(snu11)* mutants were measured by quantitative real-time PCR. Total RNAs were extracted from wild type and *egl-44(snu9)* and *egl-44(snu11)* embryos and mRNA levels of top 20 ranked genes were measured (three biological replicates for each strain).

.

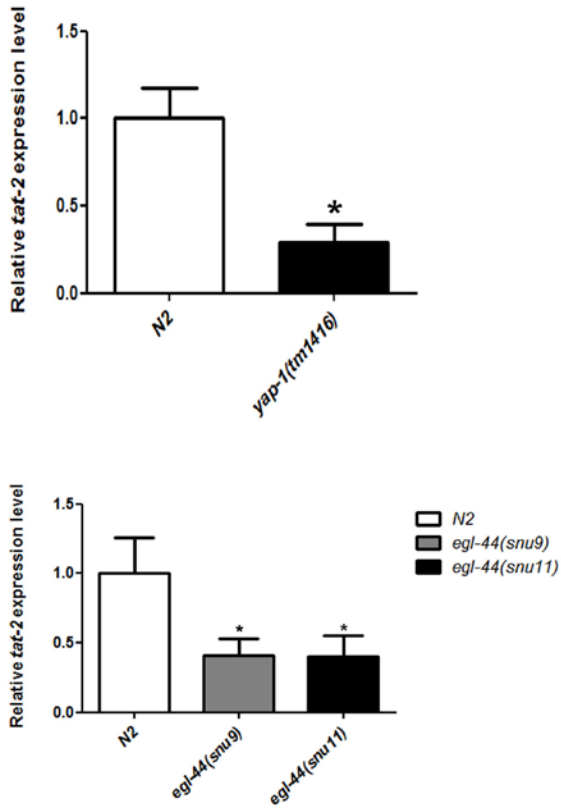

Figure 8. Relative expression levels of *tat-2* in *yap-1* and *egl-44* mutants.

Relative mRNA expression level of *tat-2*. *tat-2* expression was consistently decreased in *yap-1(tm1416)*, *egl-44(snu9)*, and *egl-44(snu11)* embryos compared to that in wild type N2 embryos. Total RNA was extracted from embryos of each mutant. The relative *tat-2* mRNA levels were measured by quantitative real time PCR. Four biological replicates were used for the test. Student's t-test was performed to measure statistical significance.

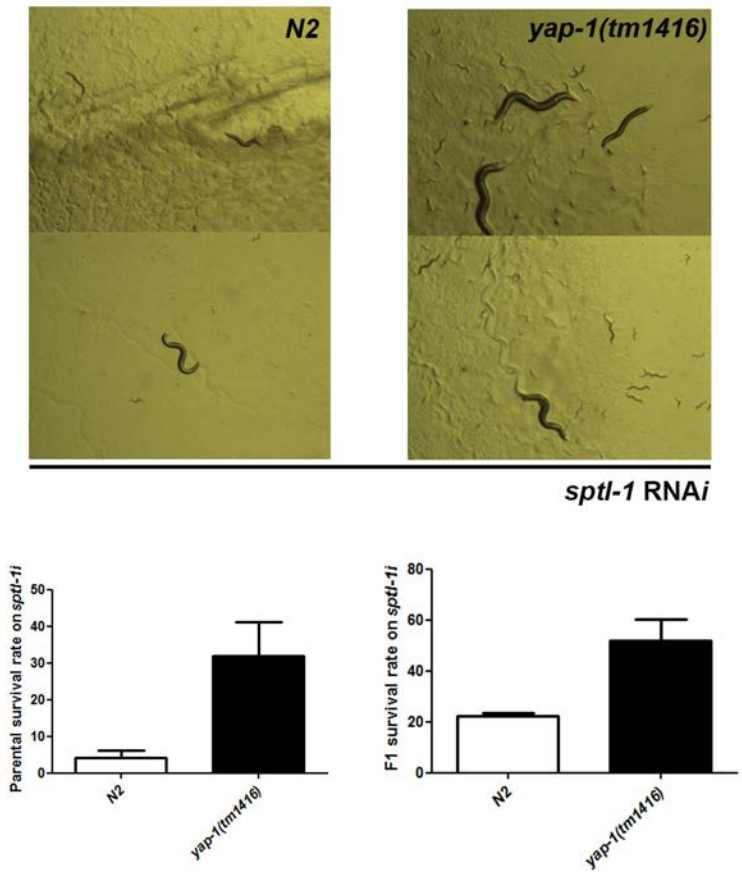

Figure 9. *yap-1* mutation suppresses lethality caused by *sptl-1* RNA*i*

yap-1 mutation suppresses *sptl-1* deficiency-mediated lethality of parents (lower, left panel) and lethality of progenies (lower, right panel).

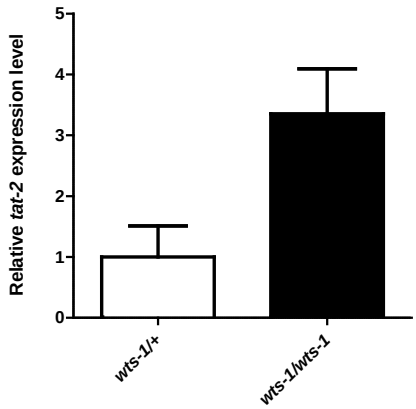

Figure 10. *wts-1* mutant has increased *tat-2*

The relative expression levels of *tat-2* were measured in *wts-1* heterozygote and *wts-1* homozygotes. In synchronized *wts-1/hT2* worms at L1 stage, *wts-1* heterozygotes and *wts-1* homozygotes were sorted using worm sorter (Union Biometrica, Inc.,).

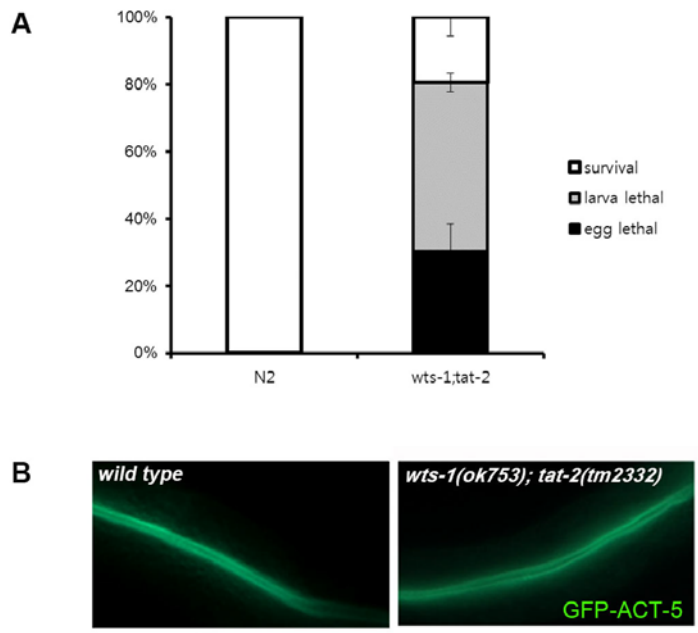

Figure 11. *tat-2(tm2332)* suppresses larval lethality of *wts-1* mutants. Phenotype analysis of *wts-1; tat-2* double mutant. Induction of *tat-2* mutation to *wts-1* mutant suppressed L1 lethality. About 20% of total hatched L1 worms of *wts1; tat2* developed to adult stages. L1 viability was measured by the same methods used earlier experiments and worms were grown at 20℃.

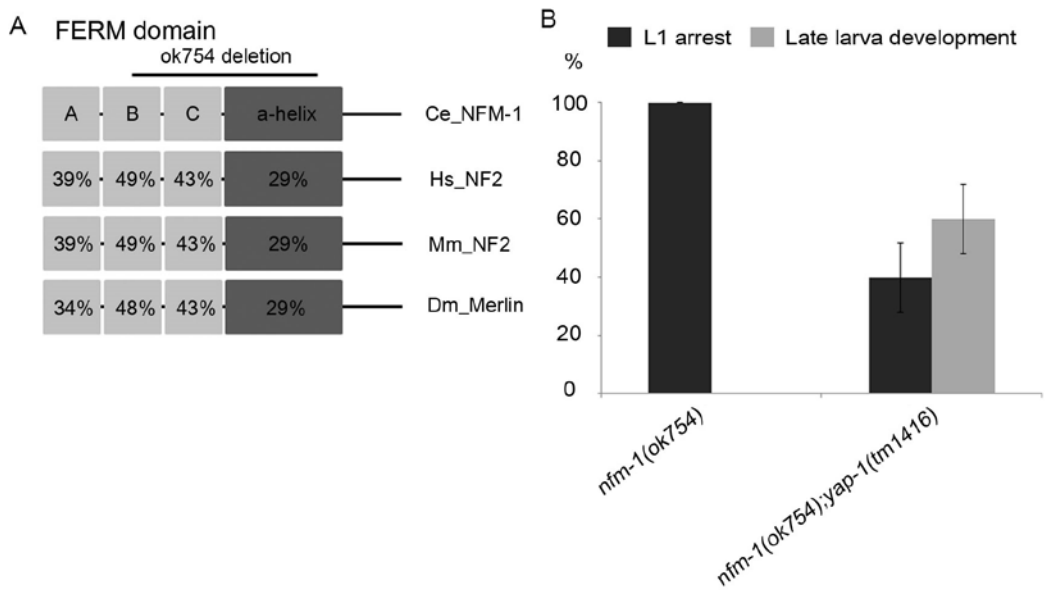

Figure 12. *yap-1* suppresses larval lethality triggered by loss of *nfm-1*, the Ce_Mer homolog. (A) The structure comparison of NF2/Merlin and NFM-1 genes. They share some common characteristics including FERM domain and the following α-helix. *nfm-1(ok754)* has a large deletion (1042 bp) in the FERM domain and α-helix (D) Phenotypic analysis of *nfm-1; yap-1*. *yap-1* mutation suppressed L1 lethality in *nfm-1* mutant; however, it failed to develop beyond the L3 stage. In collaboration with J. Kang.

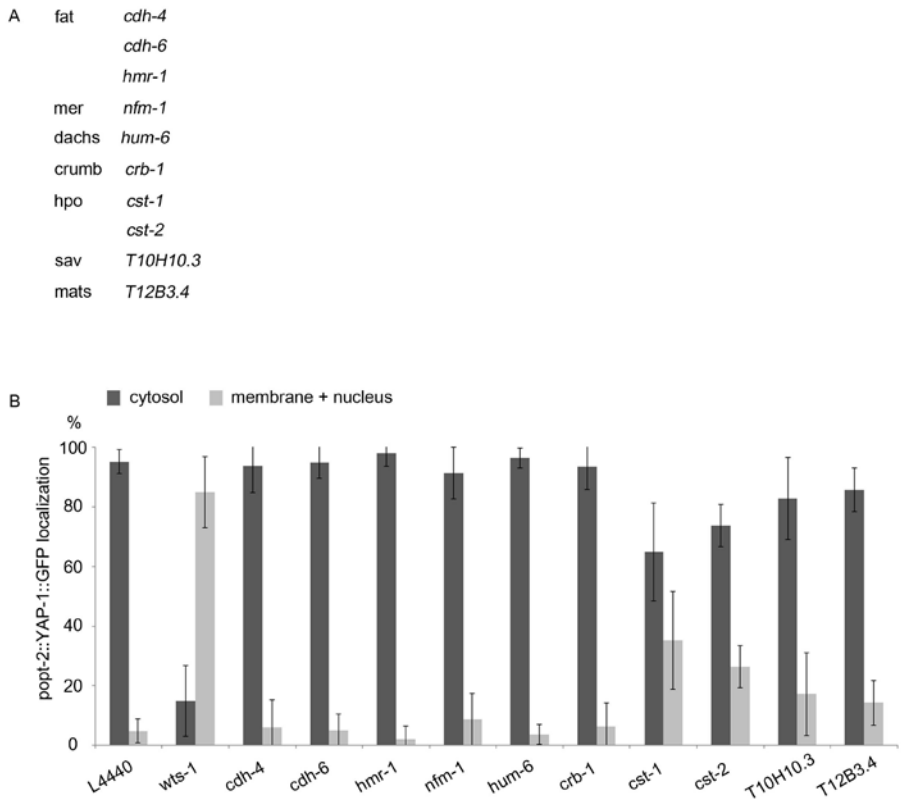

Figure 13. Subcellular localization of intestinal YAP-1 in worms in which Hpo pathway components were knocked down. (A) Putative *C. elegans* homolog genes of the Hpo pathway components. Genes were selected based on their sequence homologies (B) Analysis of subcellular distribution of YAP-1 in animals with knocked down Hpo pathway components. Only RNA*i* against to CST-1 and CST-2, the worm homolog of Hpo kinase, partially induced nuclear accumulation of YAP-1.

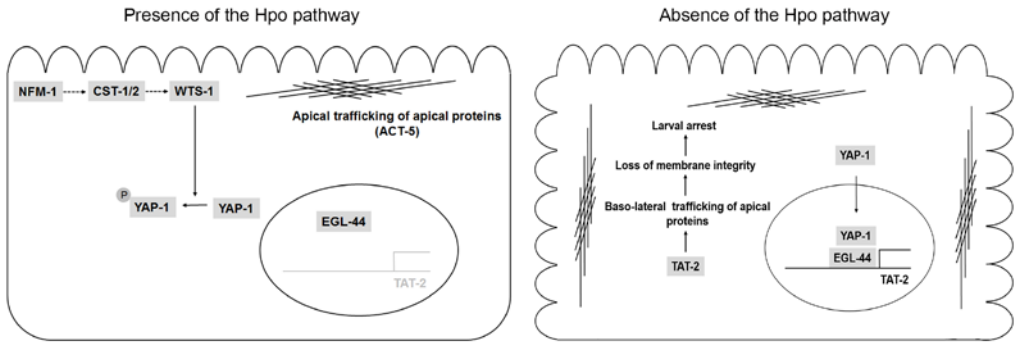

Figure 14. A working Model of the Hpo pathway in apicobasal polarity maintenance

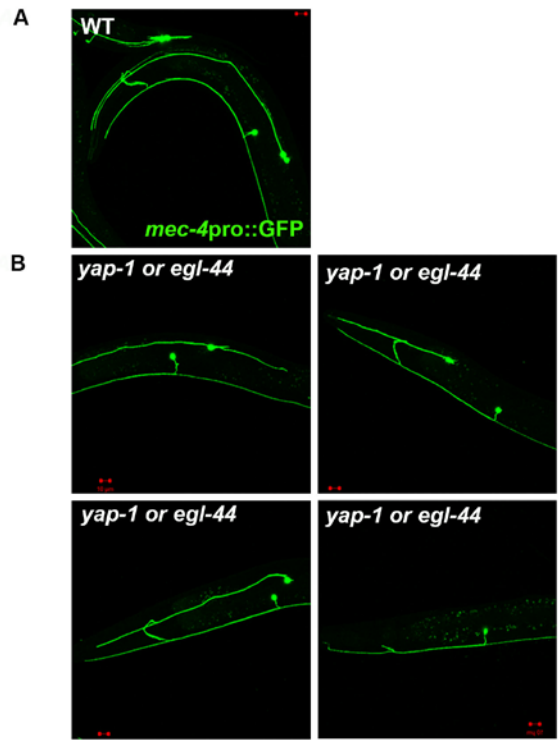

Figure 15. Defects of *yap-1* and *egl-44* mutants in neuronal development. (A) Touch receptor neurons of wild type, N2 Bristol. Touch receptor neurons are visualized with GFP under the control of *mec-4* promoter. (B) Morphological defects in *yap-1* or *egl-44* mutant backgrounds. *yap-1* or *egl-44* mutants display defects including bipolar growth, premature cell stop, neurite guidance abnormalities and loss of *mec-4* promoter expression. (L4 stage, scale bars: 10 μm)

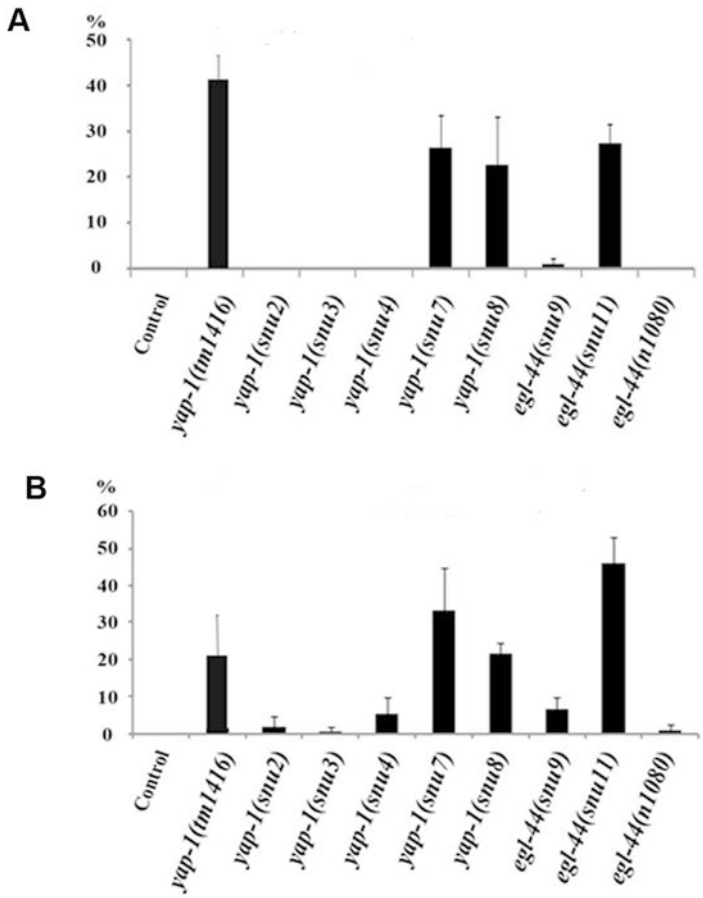

Figure 16. Bipolar outgrowth of ALM neurons in various alleles of *yap-1* and *egl-44* mutant. ALM neurons were visualized with GFP under the control of *mec-4* promoter in panel (A). ALM neurons were labeled with GFP under the control of *mec-7* promoter in panel (B). At least 20 L4 worms for each strain were observed at once. Observations were repeated for three times. The graph shows the percentage of worms have bipolar defects in ALM.

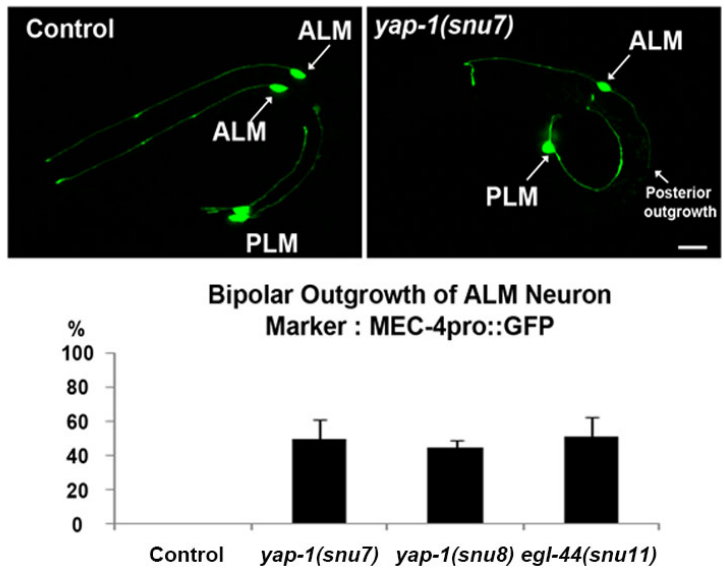

Figure 17. Bipolar outgrowth of ALM neurons in just hatched *yap-1* and *egl-44* mutant. *yap-1* or *egl-44* mutant displayed bipolar outgrowth of ALM neurons form embryos. Penetrance of phenotype of just hatched L1 were similar with those of L4 worms. Touch receptor neurons including ALM and PLM were visualized with *mec-4*pro::GFP. At least 30 just hatched L1 for each strain were used for analysis at once and observation were repeated for three times. Scale bar: 10 μm.

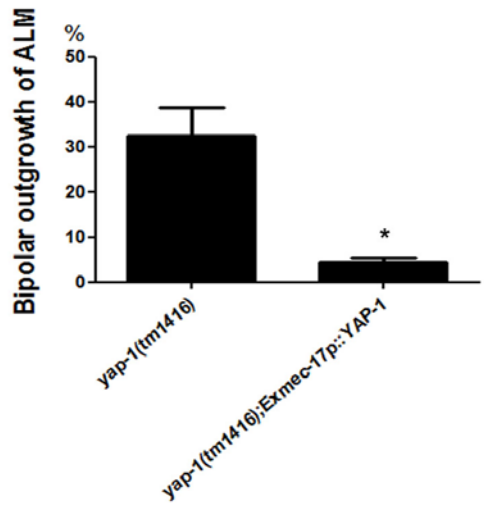

Figure 18. Touch receptor neuron-specific rescue of YAP-1 activity. Bar indicates the percentages of worms displaying bipolar outgrowth of ALM neurons. To define that YAP-1 acts in cell autonomously in asymmetric development of ALM, wild type copies of YAP-1 was expressed only in touch receptor neurons. Worms were observed at L4 stage. For one experiment, 20 animals of each strain were used, and analysis were repeated for three times. Unpaired student's T test. * $p < 0.05$.

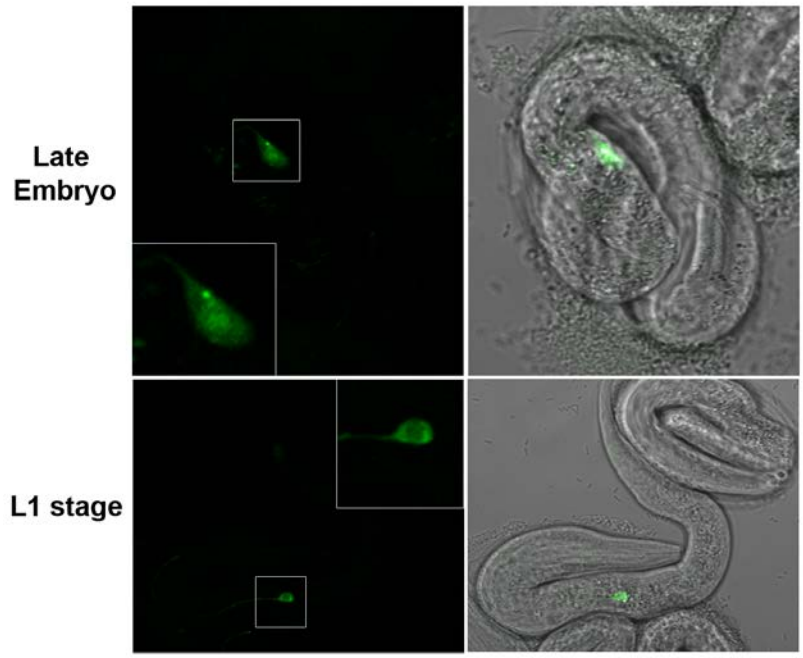

Figure 19. Subcellular localization of YAP in embryos and L1 worms. Subcellular localization of YAP-1 in ALM neurons were observed at late embryos (upper panel), and L1 worms (lower panel). GFP fused YAP-1 was expressed under the control of touch neuron specific promoter, *mec-4*.

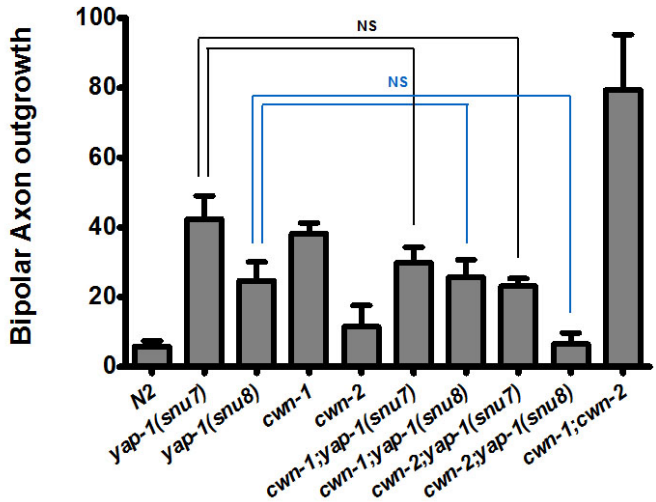

Figure 20. Genetic interactions with the Wnt pathway and YAP-1. Graph shows the percentage of animals with bipolar outgrowth of ALM neurons. Introduction of mutation in *cwn-1* or *cwn-2* into *yap-1* mutant backgrounds do not lead further increase of defects in ALM neurons. ALM neurons of each strain were observed at L4 stage. Observations were repeated for three times. Statistical significances were determined by one-way ANOVA.

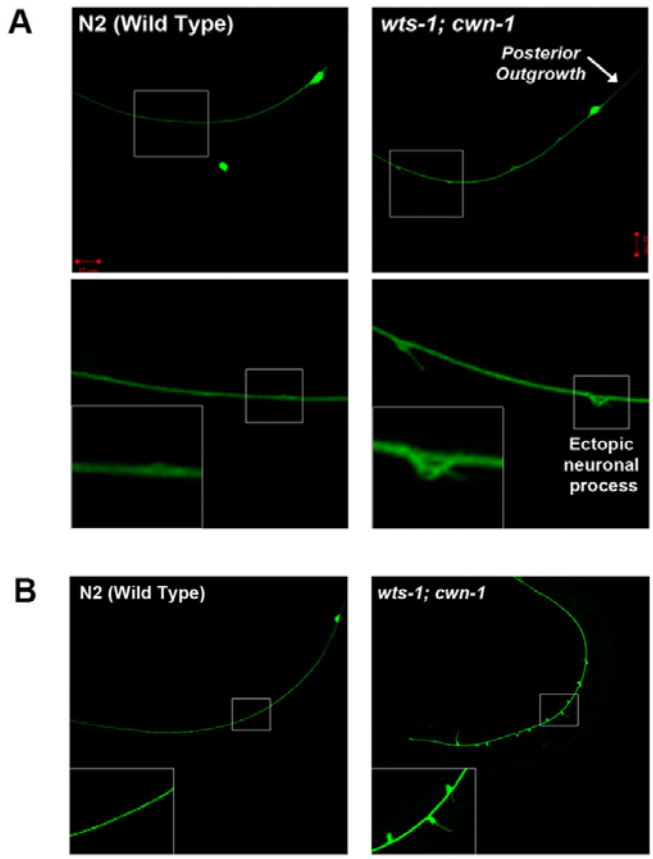

Figure 21. Ectopic branches on touch receptor neurons of *wts-1; cwn-1* double mutant (A) ALM neurons labeled with *mec-7*pro::GFP. Left panel shows intact ALM neurons in wild type. Right panel shows ectopic branches on ALM neuronal processes of *wts-1; cwn-1* double mutants. *wts-1; cwn-1* also has defects in asymmetric development of ALM neurons (white arrow). (B) PLM neurons of wild type control worms and *wts-1; cwn-1* double mutants. For all cases, 1day adult worms were observed. Scale bars: 10 μm.

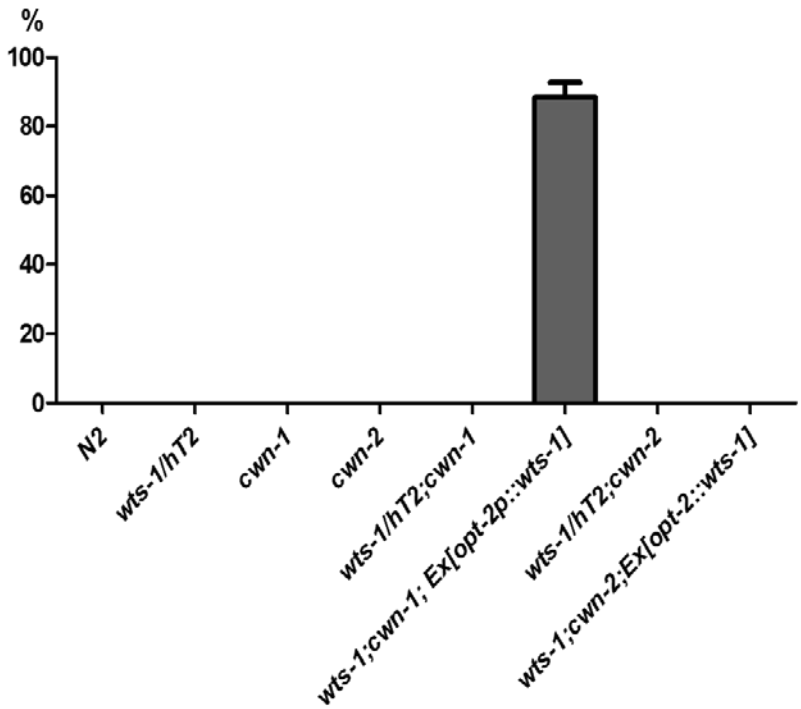

Figure 22. The frequencies of ectopic neuronal branches on touch receptor neurons in various mutant backgrounds. The graph shows the frequencies of ectopic branches on touch receptor neurons, ALM and PLM in several mutants I tested. Since *wts-1* null mutation causes organismal death, it was balanced with genetic balancer, hT2 or was rescued by wild type copies of WTS-1 expression in intestine. For all genotypes, at least 60 worms at L4 stage were observed.

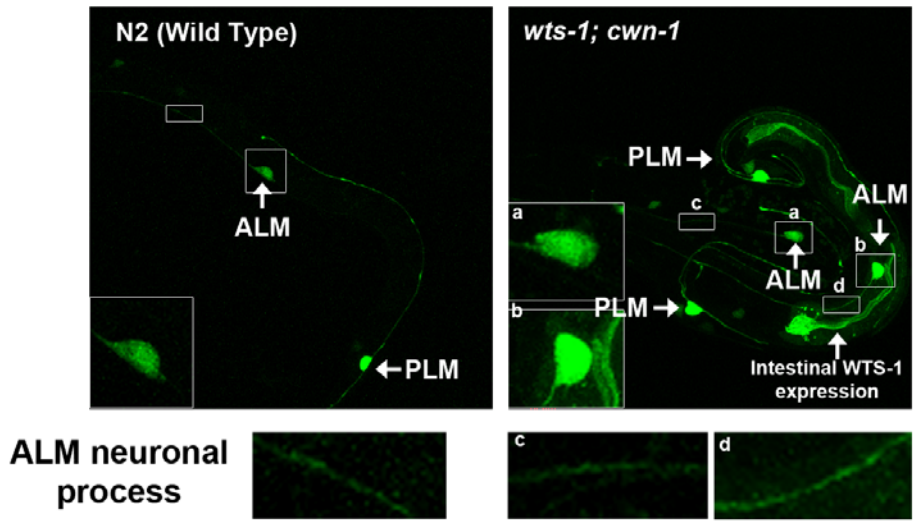

Figure 23. Intact ALM neurons in wild-type and *wts-1; cwn-1* mutant embryos. ALM neuronal morphology of wild type(left) and *wts-1; cwn-1* double mutant(right). White arrows and a, b in right panel indicate cell bodies of ALM and PLM neurons. Lower panels including c, d show magnified images of neuronal processes of wild type, N2 and *wts-1; cwn-1* double mutants.

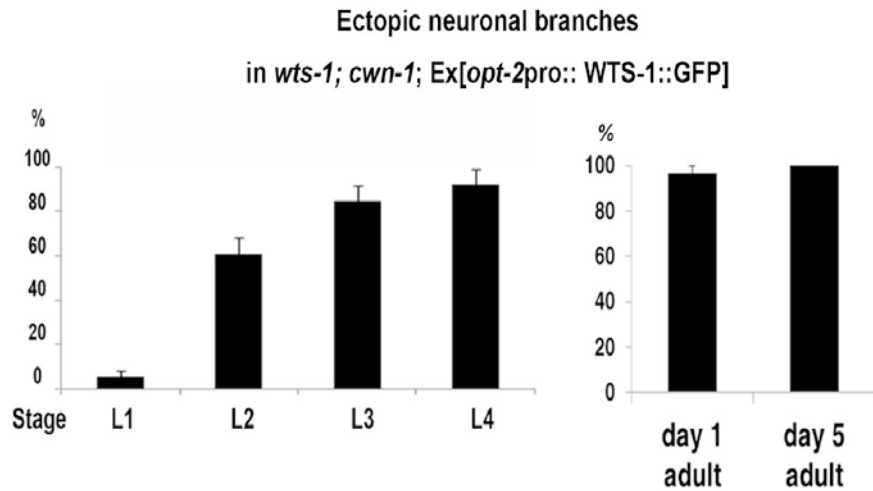

Figure 24. **The frequencies of ectopic branches of ALM neurons in *wts-1; cwn-1* double mutants in differential developmental stages**. Bars indicate percentages of worms displaying ectopic neuronal branches on ALM neurons. Worms were synchronized with standard bleaching methods, and developmental stages of worms were verified by anatomical characteristics of them. For each stage, at least 20 worms were used for analysis and analyses were repeated for three times.

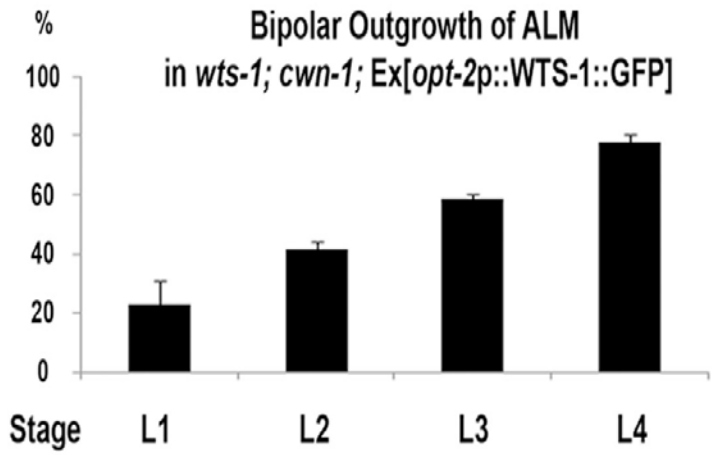

Figure 25. The frequencies of bipolar ALM neurons in *wts-1; cwn-1* double mutant in differential developmental stages. The graph shows the frequencies of worms having defects in ALM asymmetry along developmental stages. Analyses were done with same methods in Figure 11.

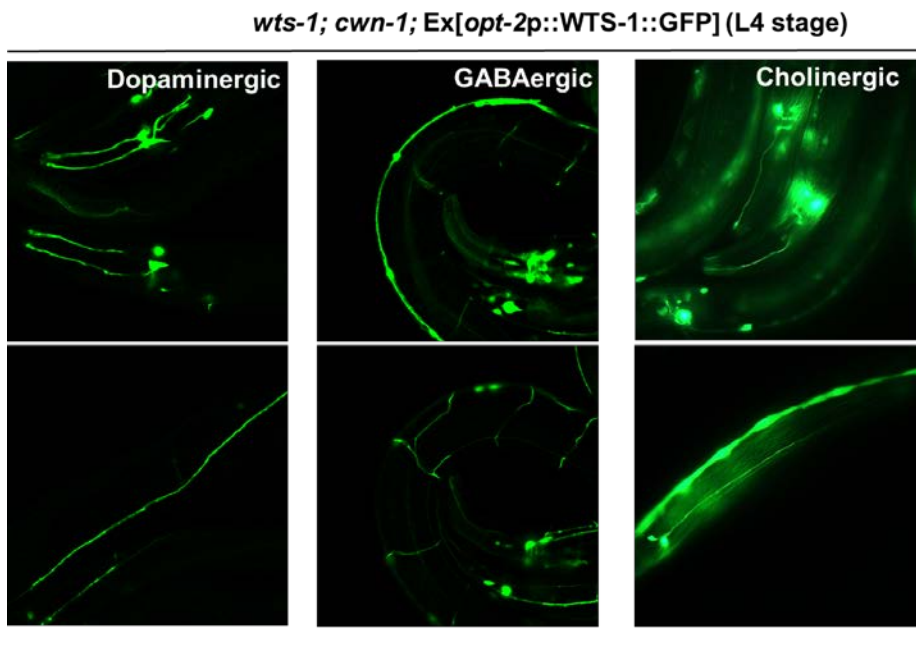

Figure 26. Intact structure of other types of neurons in *wts-1; cwn-1* double mutants. Representative images of dopaminergic neurons (left panel), GABAergic neurons (middle) and cholinergic neurons (right). Dopaminergic neurons were visualized with *dat-1*pro::GFP, GABAergic neurons were labeled with *unc-47*pro::GFP. *cho-1*pro::GFP were used for cholinergic neurons. L4 stage worms were observed.

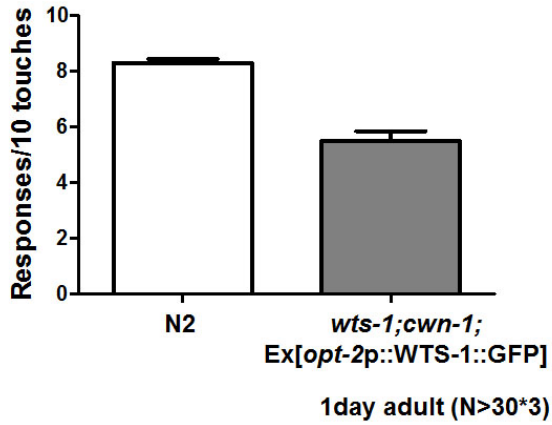

Figure 27. Touch responses of wild-type and *wts-1; cwn-1* double mutant. The graph shows the average value of touch responses per 10 touches. Gentle touch responses of individual worms were measured. More than 30 1day adult animals for each strain were used in one experiment, and analyses were repeated for three times.

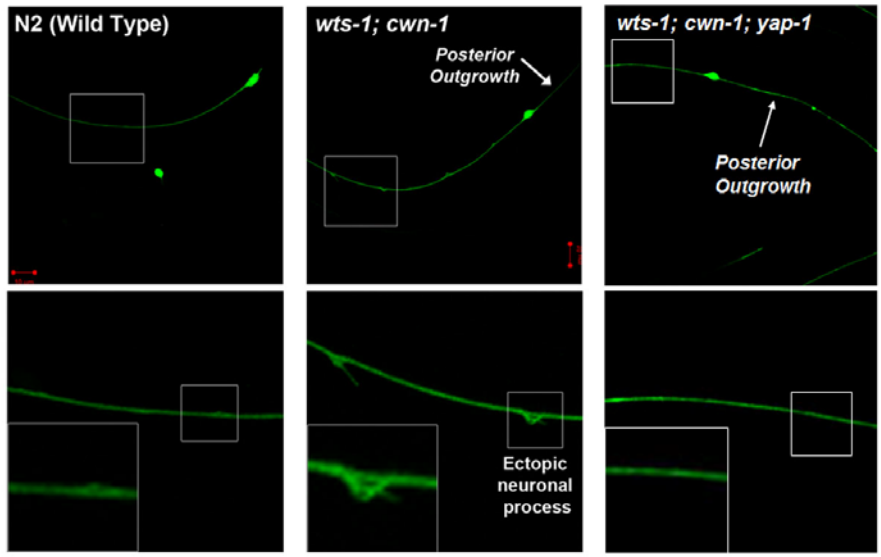

Figure 28. ***yap-1*** **mutation suppresses ectopic neuronal branches in** ***wts-1; cwn-1*** **double mutant**. ALM neurons were observed in wild type, *wts-1; cwn-1* double mutants and *wts-1; cwn-1; yap-1* triple mutants at the same developmental stage, L4. Magnified images show intact process of wild type animal (left panel), ectopically branched process in *wts-1; cwn-1* mutant (middle) and branching-suppressed, intact process of *wts-1; cwn-1; yap-1* mutant. White arrows indicate bipolar outgrowth of ALM.

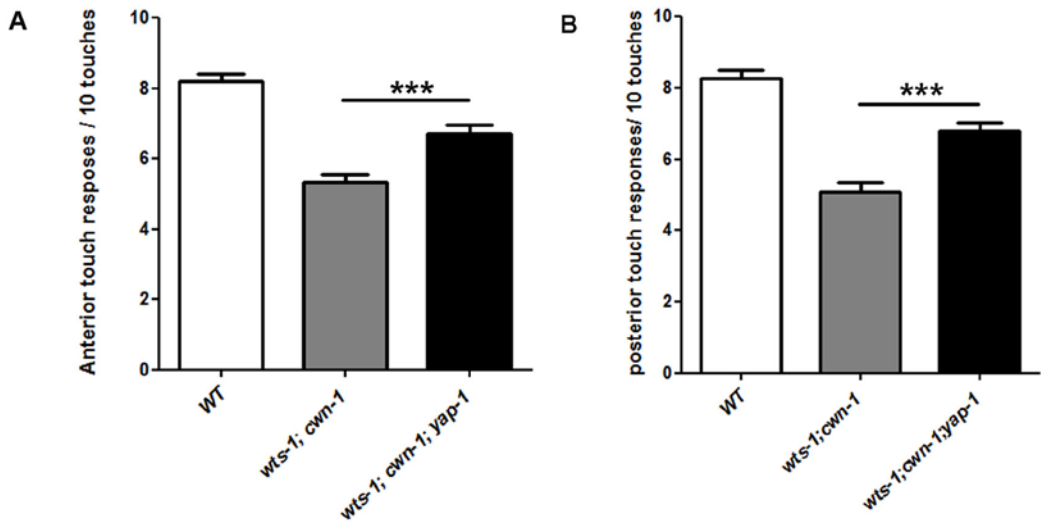

Figure 29. *yap-1* mutation partially suppresses touch insensitivity of *wts-1; cwn-1* mutants. (A) Anterior and (B) posterior touch responses were measured in wild type, *wts-1; cwn-1* mutants and *wts-1; cwn-1; yap-1* mutants. At least 30 day1 adults for each strain were used one experiment. Three times repeated. The statistical significance was determined by a one-way ANOVA with Tukey's comparison method. *** $p<0.001$

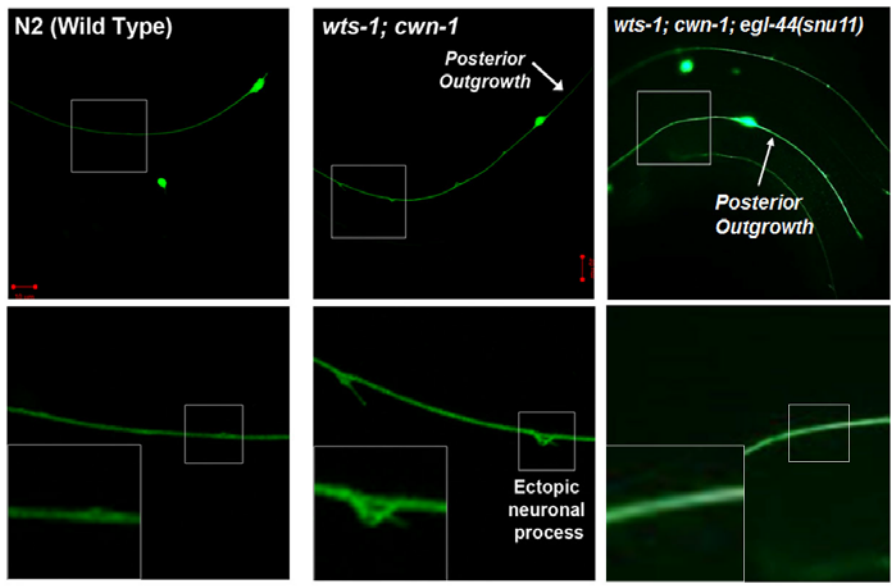

Figure 30. *egl-44* is also required to induce ectopic branches in *wts-1; cwn-1* mutants. Introduction of *egl-44* mutation into *wts-1; cwn-1* mutants also suppresses ectopic branches formation. Similar with *yap-1* mutation, *egl-44* mutation failed to suppress bipolar outgrowth of ALM neurons (white arrows)

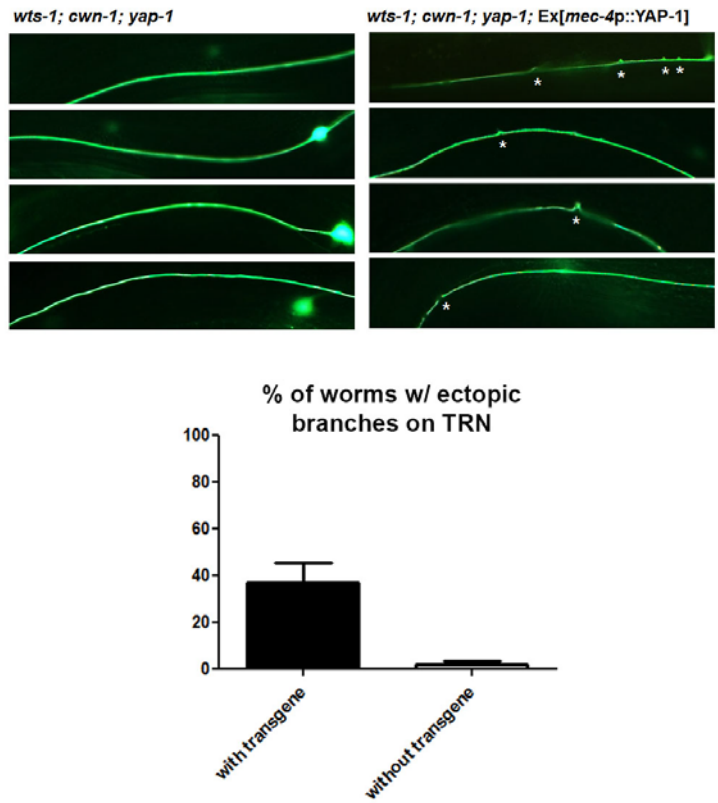

Figure 31. Touch neuron specific rescue of YAP-1 activity. Expression of YAP-1 in touch receptor neurons were sufficient to induce ectopic neuronal branches in *wts-1; cwn-1; yap-1* mutants. Asterisks indicate branching site on touch receptor neurons. Wild type copies of YAP-1 under the control of *mec-4* promoter were injected to *wts-1; cwn-1; yap-1* mutants. Progenies without injection marker were used as controls.

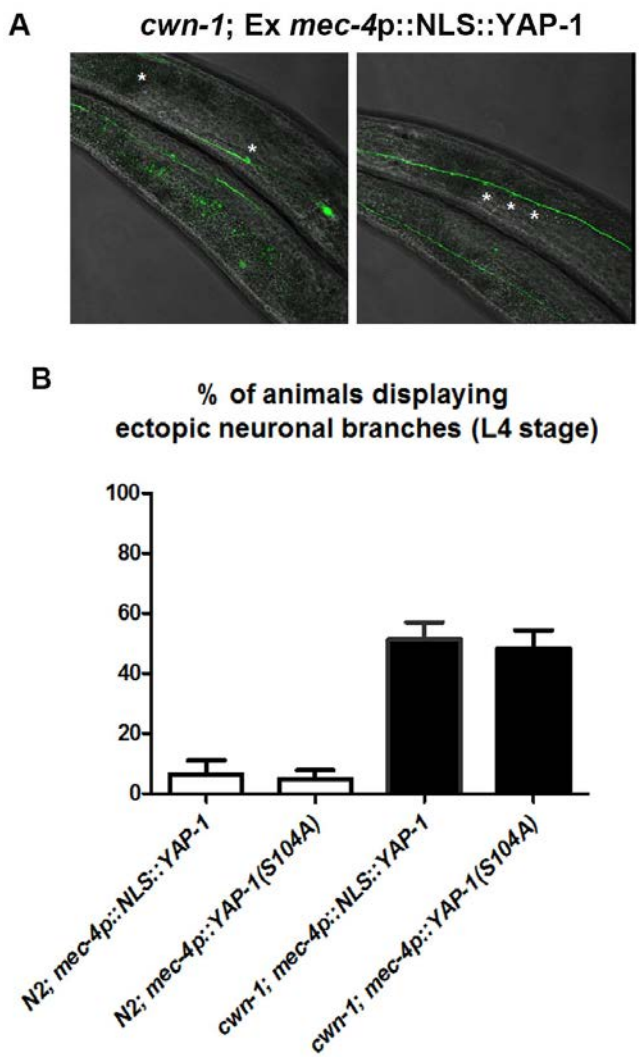

Figure 32. Genetic interaction of *cwn-1* and *yap-1* in the induction of ectopic neuronal branches. Constitutively active form of YAP-1 is not sufficient to induce ectopic branches (lower panel, first two columns). Only expression of constitutively active YAP-1 in touch receptor neurons in *cwn-1* mutant

background induces ectopic branches in ALM and PLM (asterisks in (A) and black columns in (B)). All animals were observed at L4 stage.

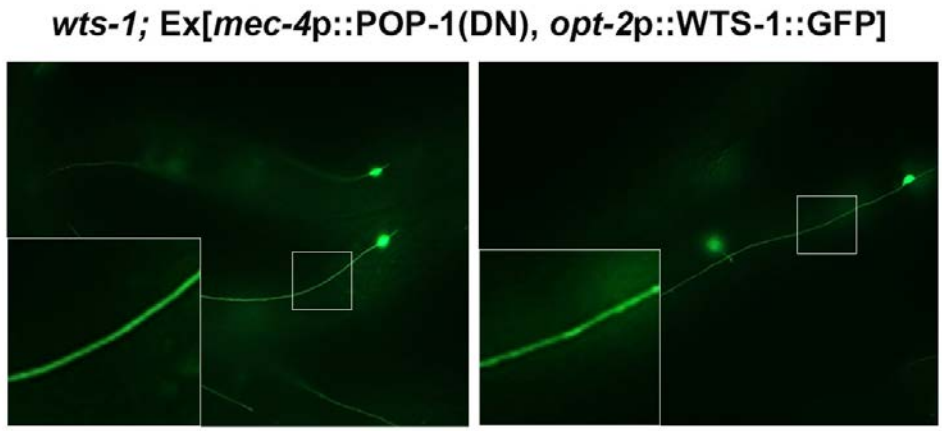

Figure 33. Touch neuron specific interferences of the canonical Wnt pathway in *wts-1* mutants. Touch neuron specific expression of dominant negative form of POP-1, the most downstream effector of the canonical Wnt pathway, in *wts-1* mutant backgrounds does not lead ectopic branches. Magnified images show intact touch neuron processes in transgenic worms. L4 worms were observed.

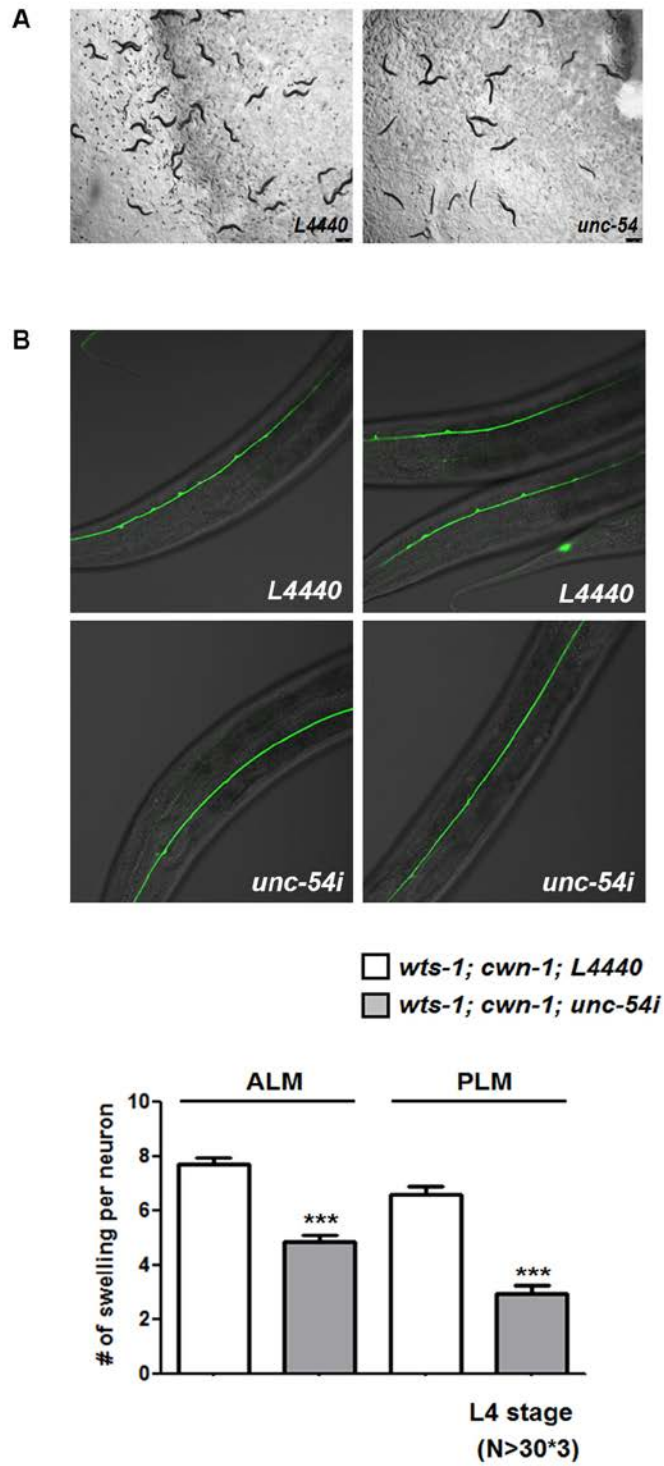
A
L4440
unc-54
B
L4440
L4440
unc-54i
unc-54i
wts-1; cwn-1; L4440
wts-1; cwn-1; unc-54i
ALM
PLM
# of swelling per neuron
10
8
6
4
2
0
***
***
L4 stage
(N>30*3)

Figure 34. Effects of *unc-54* knock down in animal movement and ectopic neuronal branches formation. (A) Un-coordinated movement triggered by *unc-54* knock down using RNA*i*. Normal movement of *wts-1; cwn-1* double mutant fed empty vector (left panel) and defective movements of *wts-1; cwn-1* double mutant fed *unc-54* RNA*i* (right panel). 4-6 L4 stage worms were transferred to either the control plates or RNA*i* plates and F1 generation worms are shown in figures. (B) Ectopic neuronal branches in empty vector fed worms (upper panel) and in *unc-54* RNA*i* fed worms (middle panel). The number of ectopic branches on ALM, PLM neurons were measured in L4 progeny worms. Statistical significances were determined by unpaired t-test. *** $p<0.001$

A

	Phenotype
unc-15	unc
unc-45	slightly unc
unc-54	severely unc
unc-89	WT
unc-95	slightly unc
unc-112	emb lethal
deb-1	WT

B

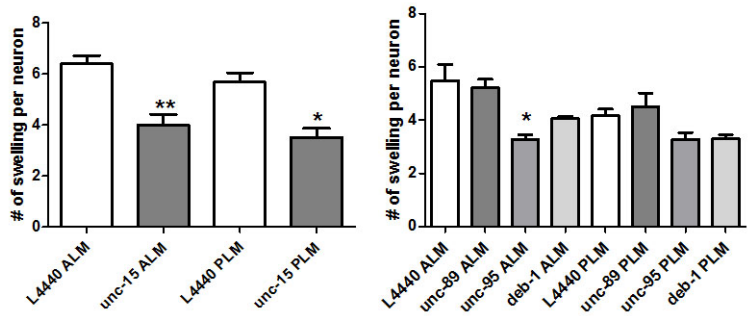

Figure 35. Knock down effects of several *unc* genes in *wts-1; cwn-1* double mutants. (A) Summarized result of the effects of *unc* genes RNA*i* on animal movements. Movement of each worm were observed in F1 generation at L4 stage. (B) The frequency of ectopic branches on ALM and PLM neurons of *wts-1; cwn-1* double mutants fed several *unc* genes RNA*i*. Statistical significances were determined by unpaired t-test. * $p<0.05$, ** $p<0.01$

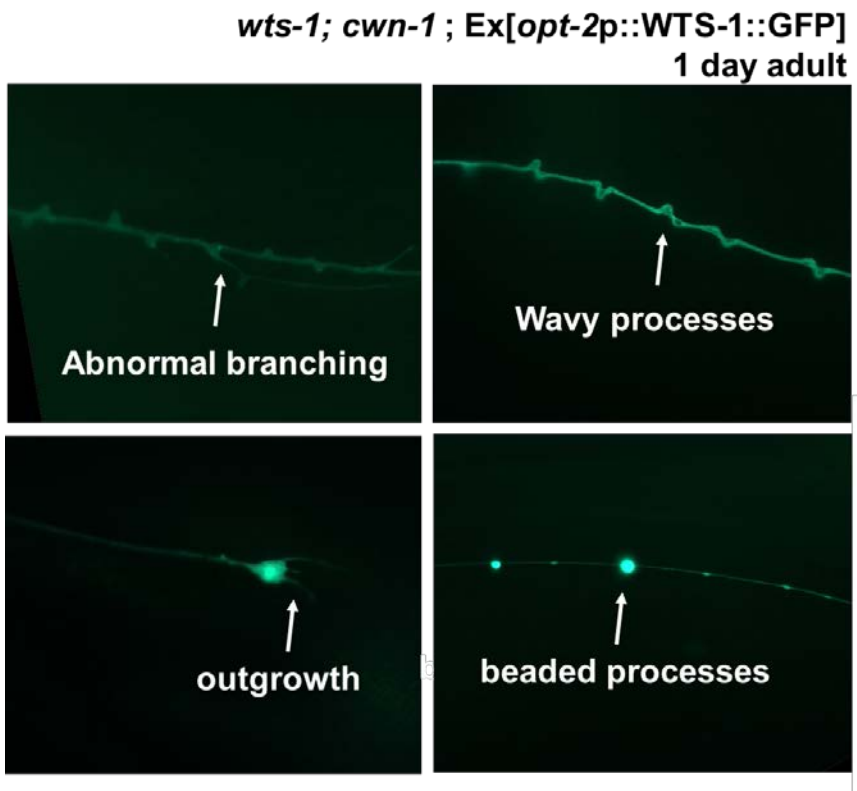

Figure 36. Age-related characteristics of neurons in *wts-1; cwn-1* mutants.

wts-1; cwn-1 mutants prematurely display all age-related features including abnormal branching, wavy processes, soma outgrowth and beaded processes on touch receptor neurons. Day1 adult worms were observed and white arrows indicate abnormal structures known to be related with aging.

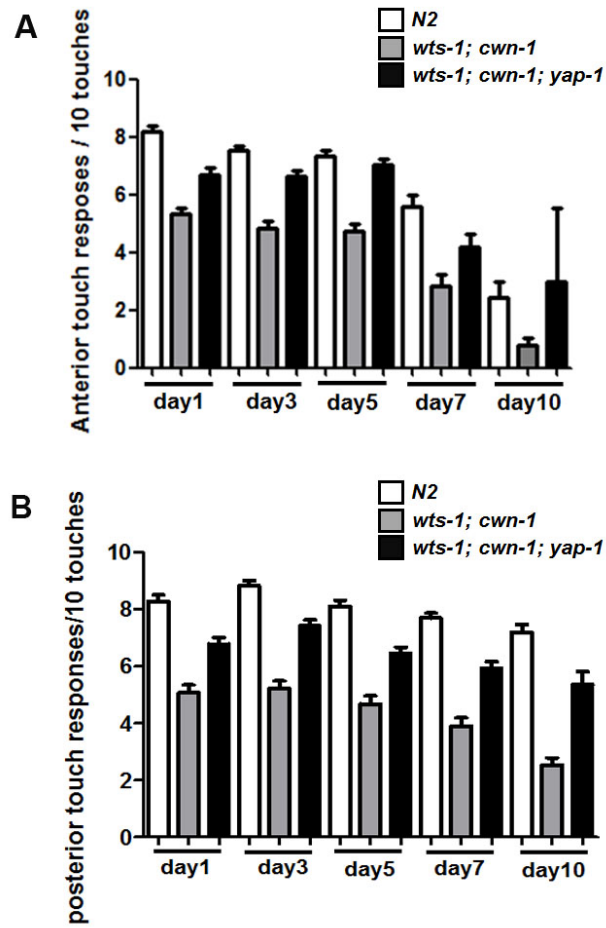

Figure 37. Analysis of touch responses with aging. (A) Anterior and (B) posterior touch responses of each strains were measured in 1, 3, 5, 7, 10 day adults. White column show the responses of wild type worms, gray and black columns indicates those of *wts-1; cwn-1* mutants and *wts-1; cwn-1; yap-1* mutant, respectively. For each strain in each day, at least 20 worms were tested, and analyses were done three times.

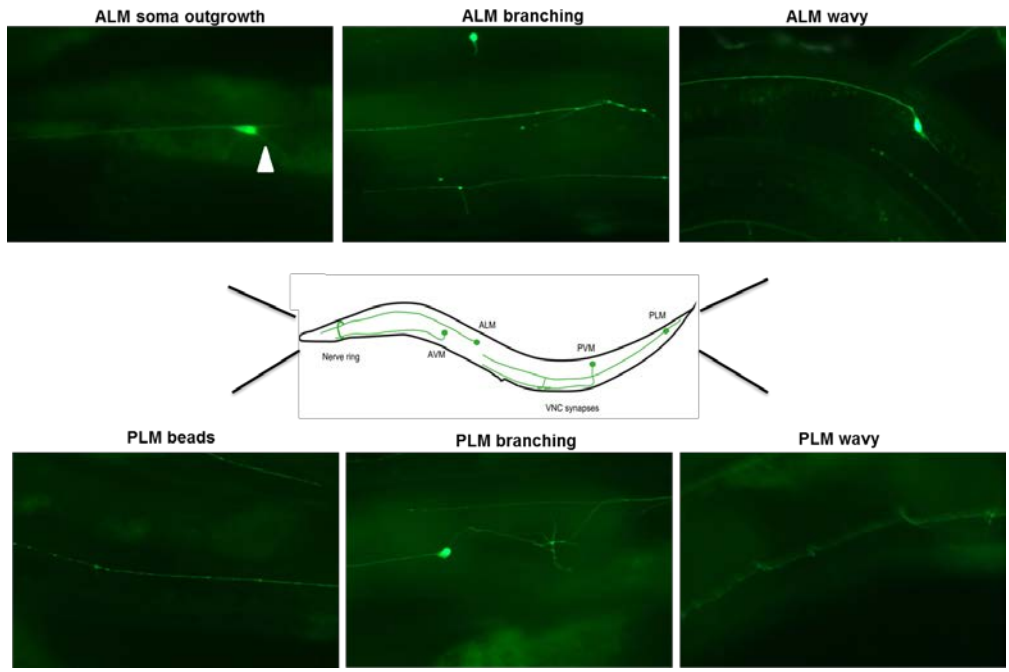

Figure 38. Morphological characteristics of aged neurons

Representative images of various morphological characteristics of aged neurons. TRNs were labeled with *mec-4*pro::GFP. All images were acquired from aged wild type worms (>10 days).

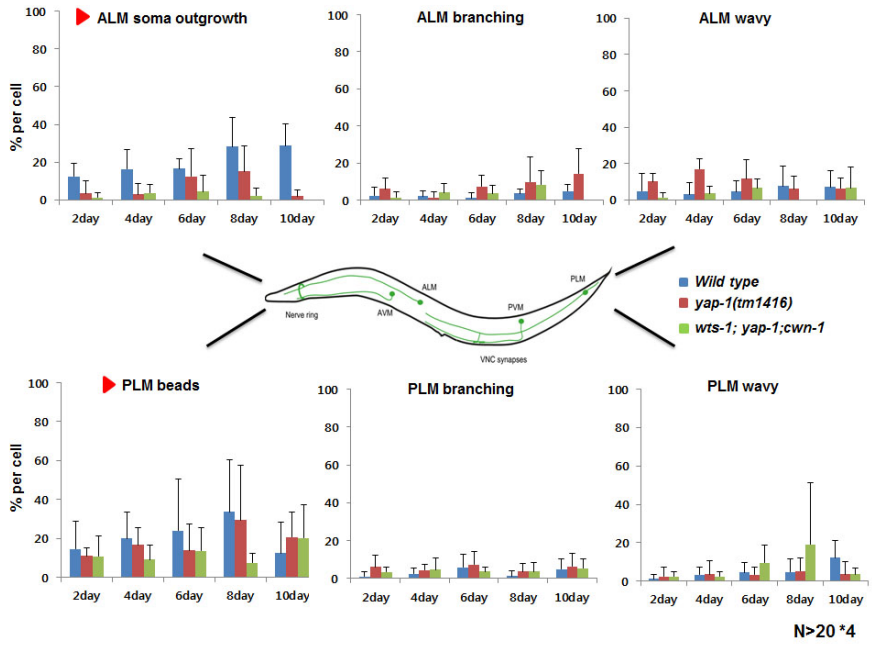

Figure 39. Morphological characteristics of aged neurons in *yap-1* mutant

The frequency of each morphological characteristics of aged neurons were measured. Worms were synchronized by standard bleaching methods. In X-axis, n day means they were in n day of their adulthood.

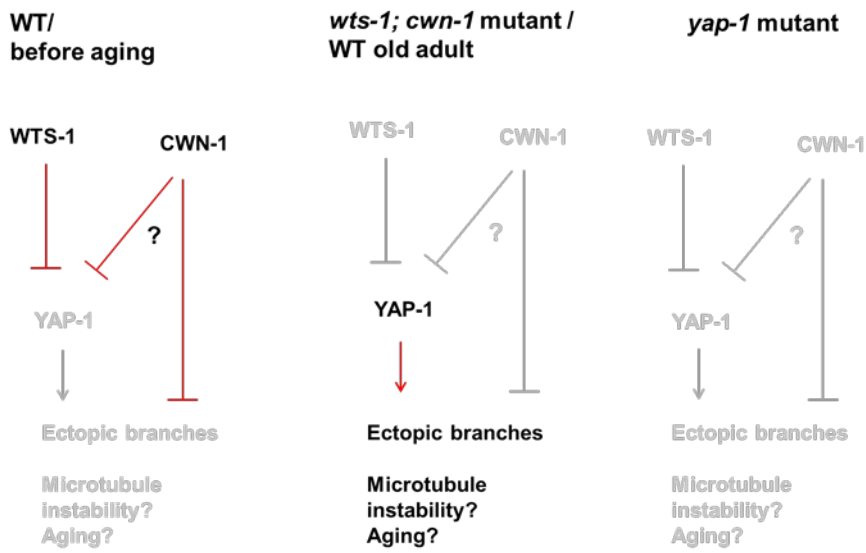

Figure 40. A working model

	Average Fold Change	P-Value	ORF name	*Gene name*	Description
1	0.320817	0.011945	F32A7.6	*aex-5*	An ortholog of calcium-dependent serine endoproteinases, expressed in muscle cells
2	0.379255	0.02387	F15E11.13	*pud-1.1*	Unknown function, upregulated in *daf2(gf)*, expressed in intestine, hypodermis
3	0.558828	0.015171	F37A4.3		Enriched in germline precursor cell and hypodermis
4	0.578682	0.015112	H22K11.4	*sgca-1*	An ortholog of the human gene SARCOGLYCAN, expressed in muscle
5	0.639495	0.040136	Y4C6B.3		An ortholog of members of the human SLC (Solute carriers) family
6	0.644521	0.031119	T25G12.9		Transposon origin, removed from *C. elegans* protein set. * excluded from our analysis.
7	0.64938	0.042419	F28H6.1	*akt-2*	AKT(S/T kinase), expressed in pharynx, several neurons
8	0.651203	0.032054	F58G11.1	*letm-1*	An ortholog of human LETM2, ubiquitously expressed in intestine, neurons
9	0.661877	0.004028	F54F2.7		An ortholog of human FAM206A, involved in locomotion
10	0.663227	0.041844	C16A11.9	*fbxc-43*	F-box C protein
11	0.66922	0.034881	C52E12.4	*ist-6*	An ortholog of human DENND5B, expressed in head neurons
12	0.68023	0.043633	F11C1.1		An ortholog of human CHCHD4
13	0.682807	0.016116	H13N06.2		

14	0.686958	0.012506	K10B2.2	*ctsa-1*	An ortholog of human CTSA, predicted to have serine-type carboxypeptidase activity
15	0.689195	0.003127	Y39B6A.33		An ortholog of mammalian GLTSCR2/PICT1, expressed in body wall muscle
16	0.691668	0.020361	H06H21.10	*tat-2*	Putative P-type ATPase, expressed in pharyngeal cell, intestine
17	0.698465	0.020347	ZC434.3		
18	0.711247	0.048998	T19D12.7	*oig-8*	Expressed in excretory cell, and several neuron
19	0.713881	0.037381	F56C9.7		DUF1261 domain, expressed in intestine
20	0.725492	0.030913	R193.2		
21	0.73886	0.036512	D1025.4	*nspc-20*	Expressed in intestine
22	0.738942	0.041445	R03G5.6		Expressed in Dopaminergic neuron
23	0.739968	0.046336	Y32F6A.5		An ortholog of human SCPEP1 (serine carboxypeptidase 1);
24	0.740127	0.019065	K04C1.4	*mlc-8*	An ortholog of members of the human MYL (Myosin light chains)
25	0.741041	0.045371	DY3.3	*hlh-16*	An ortholog of human OLIG1 (oligodendrocyte transcription factor 1), expressed in several neurons
26	0.752337	0.039948	T22B7.1	*egl-13*	SOX domain transcription factor, expressed in body wall muscle
27	0.755058	6.01E-04	F22F4.1		
28	0.758606	0.025408		*che-13*	Involved in cilia structure maintenance,

			F59C6.7		expressed in ciliated sensory neurons
29	0.759251	0.034832	T03G6.3		An ortholog of human ENPP6, expressed in body wall muscle, vulva muscle

	Average Fold Change	P-Value	ORF name	Gene name	Description
1	3.798170243	0.00667	H11L12.1		
2	3.237735007	0.01587	F47G4.4		Paralog of MEI-2, expressed in ciliated cells
3	2.874796969	0.04843	F26A1.8		hypodemrmis, neurons
4	2.178378092	0.019599	Y55B1BM.1	*stim-1*	An ortholog of STIM1, a putative calcium sensor of ER
5	1.977510254	0.03369	Y39A1A.9		An ortholog of human C17orf104
6	1.874846671	0.022883	C36C9.1	*meg-4*	Involved in P granule assembly, expressed pharynx
7	1.819210897	0.025027	K06A9.2		F-box protein
8	1.814827825	0.041835	F49E12.1	*skpo-1*	Predicted to have heme binding activity and peroxidase activity
9	1.756865247	0.018247	pqn72		Predicted to contain a glutamine/asparagine-rich domain
10	1.736272617	0.013073	F39D8.3		
11	1.719518165	0.023733	pqn91		Predicted to contain a glutamine/asparagine-rich domain
12	1.707252705	0.010207	T19H12.9	*ugt-12*	An ortholog of human UGT3A2 (UDP glycosyltransferase 3 family

13	1.64639257	0.01672	DC2.7	*kin-33*	An ortholog of human CHEK1
14	1.620972927	0.022088	F58G1.1		
15	1.606301115	0.003514	C06G3.2	*klp-18*	Kinesin motor protein
16	1.569667482	0.017891	K07A9.2	*cmk-1*	Ca+2/calmodulin-dependent protein kinase I (CaMK1), expressed in intestine and nervous system
17	1.547598449	0.016443	T05E11.8		
18	1.541338416	0.010039	C01C7.1	*ark-1*	A homolog of the nonreceptor tyrosine kinase ACK
19	1.529836518	0.049756	T07D1.3		Expressed in mechanosensory neurons
20	1.509310668	0.00914	T05B4.4		Pseudogene
21	1.501722272	0.024091	F53B7.4		
22	1.490892345	0.001891	ZK154.6		
23	1.482809791	0.049555	F56C11.3		An ortholog of human GFER (growth factor, augmenter of liver regeneration), expressed in pharynx and body wall muscle
24	1.477134425	2.98E-04	Y39B6A.42		
25	1.444970812	0.014734	T04B2.5	*ipla-7*	Phospholipase A2, expressed in intestine and pharynx
26	1.436321867	0.034685	C02F5.6	*henn-1*	An ortholog of human HENMT1(HEN1 methyltransferase 1), expressed in germline and somatic cells
27	1.436026615	0.04248	K02E2.4	*ins-35*	Insulin-related peptides, expressed in chemosensory neurons and intestine

28	1.413174161	0.04906	F49E12.9	*drd-1*	An ortholog of human FAXDC2 fatty acid hydroxylase domain containing 2), expressed in intestine
29	1.398690556	0.020844	W03F9.5	*ttb-1*	An ortholog of human GTF2B (general transcription factor IIB)
30	1.397883625	0.049615	R06C7.5	*adsl-1*	An ortholog of the human gene ADSL
31	1.397439688	0.039337	T16G1.9		An ortholog of human BARD1 (BRCA1 associated RING domain 1)
32	1.397406587	0.017579	K10D2.1		An ortholog of human HIRA (histone cell cycle regulator)
33	1.390562423	0.048425	Y54G11A.2		An ortholog of human CCDC25 (coiled-coil domain containing 25), expressed in intestine and pharynx
34	1.379353843	0.020611	C03A7.11	*ugt-51*	An ortholog of human UGT3A2 (UDP glycosyltransferase 3 family, polypeptide A2)
35	1.378052477	0.015343	T23G4.3		Expressed in germline precursor cell and DA, VA neurons
36	1.375970497	0.03187	Y46D2A.2		Expressed in intestine, PVD, OLL neurons
37	1.369860897	0.002261	W01A11.1		An ortholog of human EPHX1 (epoxide hydrolase 1), expressed in various tissues including intestine and reproductive system
38	1.364948331	0.040949	Y54H5A.2		An ortholog of human HGH1 (HGH1)
39	1.364275245	0.008916	F49E8.2		
40	1.360203382	0.006114	C38C3.5	*unc-60*	Actin depolymerizing factor, actin binding protein, expressed in embryonic muscle

41	1.354122316	0.011269	C49F5.3		
42	1.344013553	0.022573	B0511.13		An ortholog of human MPPE1 (metallophosphoesterase 1);
43	1.341566644	0.004319	T22H9.2	*atg-9*	An ortholog of human ATG9B (autophagy related 9B),
44	1.340625093	0.048429	C05D10.3	*wht-1*	ATP-binding cassette (ABC) transporter, expressed in intestine
45	1.337968899	0.041015	Y37D8A.11	*cec-7*	An ortholog of human MORF4L2 (mortality factor 4 like 2)
46	1.335687868	0.020896	PAR2.3	*aak-1*	Homologs of the catalytic alpha subunit of AMP-activated protein kinases (AMPKs)
47	1.329072479	0.00376	C27D9.1		An ortholog of members of the human FUT (Fucosyltransferases), involved in body morphogenesis
48	1.328017301	0.021152	Y52E8A.2		Predicted to have zinc ion binding activity
49	1.323955193	0.008198	D2013.3		
50	1.313432752	0.030264	Y87G2A.3	*atg-4.1*	A putative cysteine protease orthologous to the human ATG4A, expressed in intestine, renal gland cells and neurons
51	1.304450971	0.037905	F59H5.1	*gbas-1*	DUF545 motif, expressed in head neuron ganglia, intestine and hypodermal cells

Table 1. Results of microarray; list of genes whose expression was affected in the absence of YAP-1 (A) Decreased expression of genes in *yap-1(snu8)* compared to the wild type. A total of 29 genes were significantly downregulated in *yap-1(snu8).* (B)

Increased expression of genes in *yap-1(snu8)* compared to the wild type. A total of 51 genes were upregulated in *yap-1(snu8).*

References

Baumgartner, R., Poernbacher, I., Buser, N., Hafen, E., and Stocker, H. (2010). The WW domain protein Kibra acts upstream of Hippo in Drosophila. Dev Cell *18*, 309-316.

Bishop, N.A., Lu, T., and Yankner, B.A. (2010). Neural mechanisms of ageing and cognitive decline. Nature *464*, 529-535.

Boedigheimer, M.J., Nguyen, K.P., and Bryant, P.J. (1997). Expanded functions in the apical cell domain to regulate the growth rate of imaginal discs. Developmental genetics *20*, 103-110.

Brenner, S. (1974). The genetics of Caenorhabditis elegans. Genetics *77*, 71-94.

Cai, Q., Wang, W., Gao, Y., Yang, Y., Zhu, Z., and Fan, Q. (2009). Ce-wts-1 plays important roles in Caenorhabditis elegans development. FEBS Lett *583*, 3158-3164.

Cao, X., Pfaff, S.L., and Gage, F.H. (2008). YAP regulates neural progenitor cell number via the TEA domain transcription factor. Genes Dev *22*, 3320-3334.

Cavallo, R.A., Cox, R.T., Moline, M.M., Roose, J., Polevoy, G.A., Clevers, H., Peifer, M., and Bejsovec, A. (1998). Drosophila Tcf and Groucho interact to repress Wingless signalling activity. Nature *395*, 604-608.

Chalfie, M., Sulston, J.E., White, J.G., Southgate, E., Thomson, J.N., and Brenner, S. (1985). The neural circuit for touch sensitivity in Caenorhabditis elegans. J Neurosci *5*, 956-964.

Cheng, N.N., Kirby, C.M., and Kemphues, K.J. (1995). Control of cleavage spindle orientation in Caenorhabditis elegans: the role of the genes par-2 and par-3. Genetics *139*, 549-559.

Emoto, K., Parrish, J.Z., Jan, L.Y., and Jan, Y.N. (2006). The tumour suppressor Hippo acts with the NDR kinases in dendritic tiling and maintenance. Nature *443*, 210-213.

Feng, X., Degese, M.S., Iglesias-Bartolome, R., Vaque, J.P., Molinolo, A.A., Rodrigues, M., Zaidi, M.R., Ksander, B.R., Merlino, G., Sodhi, A., *et al.* (2014). Hippo-independent activation of YAP by the GNAQ uveal melanoma oncogene through a trio-regulated rho GTPase signaling circuitry. Cancer Cell *25*, 831-845.

Fernandez, L.A., Northcott, P.A., Dalton, J., Fraga, C., Ellison, D., Angers, S., Taylor, M.D., and Kenney, A.M. (2009). YAP1 is amplified and up-regulated in hedgehog-associated medulloblastomas and mediates Sonic hedgehog-driven neural precursor proliferation. Genes Dev *23*, 2729-2741.

Fullekrug, J., and Simons, K. (2004). Lipid rafts and apical membrane traffic. Annals of the New York Academy of Sciences *1014*, 164-169.

Gallegos, M.E., and Bargmann, C.I. (2004). Mechanosensory neurite termination and tiling depend on SAX-2 and the SAX-1 kinase. Neuron *44*, 239-249.

Genevet, A., Polesello, C., Blight, K., Robertson, F., Collinson, L.M., Pichaud, F., and Tapon, N. (2009). The Hippo pathway regulates apical-domain size independently of its growth-control function. J Cell Sci *122*, 2360-2370.

Genevet, A., Wehr, M.C., Brain, R., Thompson, B.J., and Tapon, N. (2010). Kibra is a regulator of the Salvador/Warts/Hippo signaling network. Dev Cell *18*, 300-308.

Gobel, V., Barrett, P.L., Hall, D.H., and Fleming, J.T. (2004). Lumen morphogenesis in C. elegans requires the membrane-cytoskeleton linker erm-1. Dev Cell *6*, 865-873.

Hamaratoglu, F., Gajewski, K., Sansores-Garcia, L., Morrison, C., Tao, C., and Halder, G. (2009). The Hippo tumor-suppressor pathway regulates apical-domain size in parallel to tissue growth. J Cell Sci *122*, 2351-2359.

Hamaratoglu, F., Willecke, M., Kango-Singh, M., Nolo, R., Hyun, E., Tao, C., Jafar-Nejad, H., and Halder, G. (2006). The tumour-suppressor genes NF2/Merlin and Expanded act through Hippo signalling to regulate cell proliferation and apoptosis. Nat Cell Biol *8*, 27-36.

Hao, J.C., Yu, T.W., Fujisawa, K., Culotti, J.G., Gengyo-Ando, K., Mitani, S., Moulder, G., Barstead, R., Tessier-Lavigne, M., and Bargmann, C.I. (2001). C. elegans slit acts in midline, dorsal-ventral, and anterior-posterior guidance via the SAX-3/Robo receptor. Neuron *32*, 25-38.

Hao, Y., Chun, A., Cheung, K., Rashidi, B., and Yang, X. (2008). Tumor suppressor LATS1 is a negative regulator of oncogene YAP. The Journal of biological chemistry *283*, 5496-5509.

Harvey, K.F., Pfleger, C.M., and Hariharan, I.K. (2003). The Drosophila Mst ortholog, hippo, restricts growth and cell proliferation and promotes apoptosis. Cell *114*, 457-467.

Hu, H., Columbus, J., Zhang, Y., Wu, D., Lian, L., Yang, S., Goodwin, J., Luczak, C., Carter, M., Chen, L., *et al.* (2004). A map of WW domain family interactions. Proteomics *4*, 643-655.

Huang, J.B., Wu, S., Barrera, J., Matthews, K., and Pan, D.J. (2005). The Hippo signaling pathway coordinately regulates cell proliferation and apoptosis by inactivating Yorkie, the Drosophila homolog of YAP. Cell *122*, 421-434.

Huang, Z., Zhang, L., Chen, Y., Zhang, H., Zhang, Q., Li, R., Ma, J., Li, Z., Yu, C., Lai, Y., *et al.* (2016). Cdc42 deficiency induces podocyte apoptosis by inhibiting the Nwasp/stress fibers/YAP pathway. Cell death & disease *7*, e2142.

Hung, T.J., and Kemphues, K.J. (1999). PAR-6 is a conserved PDZ domain-containing protein that colocalizes with PAR-3 in Caenorhabditis elegans embryos. Development *126*, 127-135.

Iwasa, H., Maimaiti, S., Kuroyanagi, H., Kawano, S., Inami, K., Timalsina, S., Ikeda, M., Nakagawa, K., and Hata, Y. (2013). Yes-associated protein homolog, YAP-1, is involved in the thermotolerance and aging in the nematode Caenorhabditis elegans. Exp Cell Res *319*, 931-945.

Izumi, Y., Hirose, T., Tamai, Y., Hirai, S., Nagashima, Y., Fujimoto, T., Tabuse, Y., Kemphues, K.J., and Ohno, S. (1998). An atypical PKC directly associates and colocalizes at the epithelial tight junction with ASIP, a mammalian homologue of Caenorhabditis elegans polarity protein PAR-3. J Cell Biol *143*, 95-106.

Kang, J. (2010). Studies on the Hippo signaling pathway in Caenorhabditis elegans. unpublished doctorial dissertation Seoual National University, Seoul, Korea

Kang, J., Shin, D., Yu, J.R., and Lee, J. (2009). Lats kinase is involved in the intestinal apical membrane integrity in the nematode Caenorhabditis elegans. Development *136*, 2705-2715.

Killeen, M.T., and Sybingco, S.S. (2008). Netrin, Slit and Wnt receptors allow axons to choose the axis of migration. Dev Biol *323*, 143-151.

Korswagen, H.C. (2002). Canonical and non-canonical Wnt signaling pathways in Caenorhabditis elegans: variations on a common signaling theme. BioEssays : news and reviews in molecular, cellular and developmental biology *24*, 801-810.

Korswagen, H.C., Herman, M.A., and Clevers, H.C. (2000). Distinct beta-catenins mediate adhesion and signalling functions in C. elegans. Nature *406*, 527-532.

Kuchinke, U., Grawe, F., and Knust, E. (1998). Control of spindle orientation in Drosophila by the Par-3-related PDZ-domain protein Bazooka. Current biology : CB *8*, 1357-1365.

Lehtinen, M.K., Yuan, Z., Boag, P.R., Yang, Y., Villen, J., Becker, E.B., DiBacco, S., de la Iglesia, N., Gygi, S., Blackwell, T.K., *et al.* (2006). A conserved MST-FOXO signaling pathway mediates oxidative-stress responses and extends life span. Cell *125*, 987-1001.

Lin, D., Edwards, A.S., Fawcett, J.P., Mbamalu, G., Scott, J.D., and Pawson, T. (2000). A mammalian PAR-3-PAR-6 complex implicated in Cdc42/Rac1 and aPKC signalling and cell polarity. Nat Cell Biol *2*, 540-547.

Mellman, I., and Nelson, W.J. (2008). Coordinated protein sorting, targeting and distribution in polarized cells. Nat Rev Mol Cell Biol *9*, 833-845.

Oh, H., Reddy, B.V., and Irvine, K.D. (2009). Phosphorylation-independent repression of Yorkie in Fat-Hippo signaling. Dev Biol *335*, 188-197.

Pan, C.L., Peng, C.Y., Chen, C.H., and McIntire, S. (2011). Genetic analysis of age-dependent defects of the Caenorhabditis elegans touch receptor neurons. Proc Natl Acad Sci U S A *108*,

9274-9279.

Parrish, J.Z., Emoto, K., Jan, L.Y., and Jan, Y.N. (2007). Polycomb genes interact with the tumor suppressor genes hippo and warts in the maintenance of Drosophila sensory neuron dendrites. Genes Dev *21*, 956-972.

Pearce, L.R., Komander, D., and Alessi, D.R. (2010). The nuts and bolts of AGC protein kinases. Nat Rev Mol Cell Biol *11*, 9-22.

Petersen, C.P., and Reddien, P.W. (2009). Wnt signaling and the polarity of the primary body axis. Cell *139*, 1056-1068.

Prasad, B.C., and Clark, S.G. (2006). Wnt signaling establishes anteroposterior neuronal polarity and requires retromer in C. elegans. Development *133*, 1757-1766.

Quinn, C.C., Pfeil, D.S., and Wadsworth, W.G. (2008). CED-10/Rac1 mediates axon guidance by regulating the asymmetric distribution of MIG-10/lamellipodin. Current biology : CB *18*, 808-813.

Reginensi, A., Scott, R.P., Gregorieff, A., Bagherie-Lachidan, M., Chung, C., Lim, D.S., Pawson, T., Wrana, J., and McNeill, H. (2013). Yap- and Cdc42-dependent nephrogenesis and morphogenesis during mouse kidney development. PLoS Genet *9*, e1003380.

Roose, J., Molenaar, M., Peterson, J., Hurenkamp, J., Brantjes, H., Moerer, P., van de Wetering, M., Destree, O., and Clevers, H. (1998). The Xenopus Wnt effector XTcf-3 interacts with Groucho-related transcriptional repressors. Nature *395*, 608-612.

Seamen, E., Blanchette, J.M., and Han, M. (2009). P-type ATPase TAT-2 negatively regulates monomethyl branched-chain fatty acid mediated function in post-embryonic growth and development in C. elegans. PLoS Genet *5*, e1000589.

Silhankova, M., and Korswagen, H.C. (2007). Migration of neuronal cells along the anterior-posterior body axis of C. elegans: Wnts are in control. Current opinion in genetics & development *17*, 320-325.

St Johnston, D., and Ahringer, J. (2010). Cell polarity in eggs and epithelia: parallels and diversity. Cell *141*, 757-774.

Tabuse, Y., Izumi, Y., Piano, F., Kemphues, K.J., Miwa, J., and Ohno, S. (1998). Atypical protein kinase C cooperates with PAR-3 to establish embryonic polarity in Caenorhabditis elegans. Development *125*, 3607-3614.

Toth, M.L., Melentijevic, I., Shah, L., Bhatia, A., Lu, K., Talwar, A., Naji, H., Ibanez-Ventoso, C., Ghose, P., Jevince, A., *et al.* (2012). Neurite sprouting and synapse deterioration in the aging Caenorhabditis elegans nervous system. J Neurosci *32*, 8778-8790.

Vassilev, A., Kaneko, K.J., Shu, H., Zhao, Y., and DePamphilis, M.L. (2001). TEAD/TEF transcription factors utilize the activation domain of YAP65, a Src/Yes-associated protein localized in the cytoplasm. Genes Dev *15*, 1229-1241.

Verde, F., Wiley, D.J., and Nurse, P. (1998). Fission yeast orb6, a ser/thr protein kinase related to mammalian rho kinase and myotonic dystrophy kinase, is required for maintenance of cell polarity and coordinates cell morphogenesis with the cell cycle. Proc Natl Acad Sci U S A *95*, 7526-7531.

Wei, X., Shimizu, T., and Lai, Z.C. (2007). Mob as tumor suppressor is activated by Hippo kinase for growth inhibition in Drosophila. EMBO J *26*, 1772-1781.

Wodarz, A., Ramrath, A., Kuchinke, U., and Knust, E. (1999). Bazooka provides an apical cue for Inscuteable localization in Drosophila neuroblasts. Nature *402*, 544-547.

Wu, J., Duggan, A., and Chalfie, M. (2001). Inhibition of touch cell fate by egl-44 and egl-46 in C. elegans. Genes Dev *15*, 789-802.

Yang, Z., and Hata, Y. (2013). What is the Hippo pathway? Is the Hippo pathway conserved in Caenorhabditis elegans? J Biochem *154*, 207-209.

Yin, F., Yu, J., Zheng, Y., Chen, Q., Zhang, N., and Pan, D. (2013). Spatial organization of Hippo signaling at the plasma membrane mediated by the tumor suppressor Merlin/NF2. Cell *154*, 1342-1355.

Yu, J., Zheng, Y., Dong, J., Klusza, S., Deng, W.M., and Pan, D. (2010). Kibra functions as a tumor suppressor protein that regulates Hippo signaling in conjunction with Merlin and Expanded. Dev Cell *18*, 288-299.

Zhang, H., Abraham, N., Khan, L.A., Hall, D.H., Fleming, J.T., and Gobel, V. (2011). Apicobasal domain identities of expanding tubular membranes depend on glycosphingolipid biosynthesis. Nat Cell Biol *13*, 1189-1201.

Zhang, N., Bai, H., David, K.K., Dong, J., Zheng, Y., Cai, J., Giovannini, M., Liu, P., Anders, R.A., and Pan, D. (2010). The Merlin/NF2 tumor suppressor functions through the YAP oncoprotein to regulate tissue homeostasis in mammals. Dev Cell *19*, 27-38.

Zhao, B., Li, L., Lu, Q., Wang, L.H., Liu, C.Y., Lei, Q., and Guan, K.L. (2011). Angiomotin is a novel Hippo pathway component that inhibits YAP oncoprotein. Genes Dev *25*, 51-63.

Zhao, B., Li, L., Tumaneng, K., Wang, C.Y., and Guan, K.L. (2010). A coordinated phosphorylation by Lats and CK1 regulates YAP stability through SCF beta-TRCP. Genes & Development *24*, 72-85.

Zhao, B., Wei, X., Li, W., Udan, R.S., Yang, Q., Kim, J., Xie, J., Ikenoue, T., Yu, J., Li, L., *et al.*

(2007). Inactivation of YAP oncoprotein by the Hippo pathway is involved in cell contact inhibition and tissue growth control. Genes Dev *21*, 2747-2761.

국문 초록

예쁜꼬마선충 유전학을 이용한

Hippo pathway의 새로운 생물학적 기능 규명 연구

이하늬

서울대학교 생명과학부

Hippo 신호전달체계는 개체의 초기 발생에서 핵심적인 역할을 담당하는 신호 전달 경로이다. 이는 세포의 분열과 사멸을 조절함으로써 기관 크기의 항상성을 유지하며, 또한 극성 세포의 분화를 매개하는 것으로 알려져 있다. 예쁜꼬마선충에서 Hippo 신호전달체계의 몇 가지 구성 유전자와 그들 간의 유전적 상호작용은 보고되었지만, Hippo 신호전달체계의 생리학적인 기능 자체는 비교적 잘 밝혀지지 않았다. 본 연구는 다양한 유전학적 방법론을 이용하여, 예쁜꼬마선충 장 세포막의 극성 유지와 신경세포의 구조 안전성에 Hippo 신호전달체계가 기능함을 밝혔다.

극성 상피 세포들은 구조적, 기능적으로 구분되는 도메인을 가지고 있으며 이는 발생 과정에서 철저히 유지된다. 진화적으로 보존된 여러 극성 형성 인자들이 밝혀졌으나, 성장하는 막에서 극성이 유지되는 기작은 완전히 이해하지 못하고 있다. 본 연구는 유전학적 스크리닝을 통하여 진화적으로 보존된 NFM-1-WTS-1-YAP-1 신호전달 경로가 P형 ATPase인 *tat-2*의 전사를 조절함으로써 장 세포막의 극성 유지에

관여함을 밝혔다. Hippo 신호전달체계에 의한 *tat-2* 조절은 장 세포막의 정체성을 유지하는데 중요하며, 이것은 성장하고 있는 막에서 새롭게 합성된 단백질들이 잘 분류되는 것을 도와, 궁극적으로 성장하는 세포막의 극성을 유지한다.

나아가 본 연구는 예쁜꼬마선충에서 Hippo 신호전달체계가 신경 세포에서 기능함을 밝혔다. YAP/Yki의 상동 단백질인 *yap-1*은 신경세포의 비 대칭적인 발생에 관여한다. 또한 Hippo 신호전달체계가 신경세포의 발생 뿐 아니라, 구조적 완전성을 유지하는 데에도 필요함을 밝혔다. Hippo 신호전달체계와 Wnt 신호전달체계가 망가진 선충은 신경세포 특이적으로 지나치게 빠른 구조적, 기능적 손실을 보였다. 신경세포의 구조와 기능이 망가지는 것이 노화의 특징임을 고려할 때, 본 연구는 신경세포 노화의 분자적 기전을 이해하는 데 기여할 것이다.

요약하면, 본 연구는 예쁜꼬마선충의 Hippo 신호전달체계의 장과 신경세포에서의 발생학적 기능에 대해 밝혔으며, 신경세포의 구조 유지 측면에서 발생 후에 Hippo 신호전달체계가 어떤 역할을 하는지 규명하였다.

주요어: 예쁜꼬마선충, Hippo 신호전달체계, 장세포 극성, TAT-2, 신경세포의 구조 유지, Wnt 신호전달체계

학번: 2009-20352